FACULTY OF INFORMATION TECHNOLOGY AND ELECTRICAL ENGINEERING

DEGREE PROGRAMME IN WIRELESS COMMUNICATIONS ENGINEERING

MASTER'S THESIS

Design and implementation of a light-based IoT (LIoT) node using printed electronics

Author	Malalgodage Amila Nilantha Perera
Supervisor	Prof. Marcos Katz
Second Supervisor	Dr. Roshan Godaliyadda
Technical Advisor	Prof. Juha Häkkinen

June 2020

Perera M. (2020) Design and implementation of a light-based IoT (LIoT) node using printed electronics. University of Oulu, Faculty of Information Technology and Electrical Engineering, Degree Programme in Wireless Communications Engineering. Master's Thesis, 76p.

ABSTRACT

The recent exponential growth of new radio frequency (RF) based applications such as internet of things (IoT) technology is creating a huge bandwidth demand in the already congested RF spectrum. Meanwhile, visible light communication (VLC) is emerging as a technology which can be used as an alternative wireless communications solution which makes no use of the radio spectrum. In addition, continuously powering up the massively deployed IoT nodes is becoming a challenge when it comes to maintenance costs. Development of energy autonomous IoT nodes would certainly assist to solve the energy challenge. Previous work shows that renewable energy sources can be utilized to address the energy requirement of IoT nodes. Under this context, we have developed a light-based energy autonomous IoT (LIoT) prototype. This thesis presents a feasibility study and proof of concept of LIoT, including design, implementation and validation of LIoT nodes and a transmitter unit. Furthermore, the ability of multiuser communication using VLC as well as indoor light-based energy harvesting were demonstrated and tested in this thesis. To make the concept of LIoT more attractive from an implementation standpoint, and to create a future-looking solution, printed electronics (PE) technology was used as a part of the implementation. Two key components of the prototype were based on PE technology, photovoltaic cells used to harvest energy, and displays used to exhibit information transmitted to the LIoT node. In the future, when PE technology becomes more mature, very low-cost, small form-factor and environmentally friendly LIoT nodes could be implemented on thin substrates. A wide array of possible applications can be created combining the concept of light-based IoT with printed electronics. The proposed LIoT concept shows great promise as an enabling technology for 6G.

Key words: LIoT, VLC, IoT, Printed electronics, Indoor energy harvesting, Energy autonomous, 6G.

TABLE OF CONTENTS

FOREWORD

This thesis is focused on feasibility study and implementation of a prototype using the concept of light-based energy autonomous IoT node (LIoT) with printed electronics. The research work carried at the Centre for Wireless Communications (CWC), University of Oulu, Finland and it was funded under the 6G flagship program.

First, I would like to extend my sincere gratitude to my main supervisor Prof. Marcos Katz for creating this fascinating concept with the combination of three different technologies such as visible light communication, printed electronics and indoor energy harvesting. With his valuable support and guidance, I was able to complete this thesis work as planned. Next, I would like to thank my second supervisor from University of Peradeniya, Dr. Roshan Godaliyadda for providing his valuable comments and support on my thesis work. I also thank to my technical supervisor Prof. Juha Häkkinen for giving his valuable technical advises throughout the implementation work. I am also express my sincere gratitude to Dr. Himal Suraweera and Prof. Nandana Rajatheva for promptly helping me throughout the journey of double degree master's program. Furthermore, I would like to express my gratitude for Jari Sillanpää from CWC and Esko Strömmer from VTT Technical Research Centre of Finland, for timely arranging and providing all required components for the prototype.

Finally, I would like to express my humble gratitude my parents and my brother for giving courage, love, immense support throughout this journey. Without their courage and support this entire academic carrier away from home would not have been possible.

Oulu, June 06, 2020

Malalgodage Amila Nilantha Perera

LIST OF ABBREVIATIONS AND SYMBOLS

ADC	analogue to digital converter
ASCII	American standard code for information interchange
AGC	automatic gain control amplifier
APD	avalanche photo detector
BER	bit error rate
COB	chip on board
CSK	colour shift keying
CIJ	continues ink jet
DC	direct current
D2D	device to device
D2E	device to everything
DoD	drops on demand
eMBB	enhanced mobile broadband
eMTC	enhanced machine type communications
FHE	flexible hybrid electronics
GPIO	general purposes, input, output
IC	integrated circuit
IR	infrared
ID	identification
IoT	internet of things
IGMS	infrastructure and geophysical monitoring systems
IDE	integrated development environment
LiFi	light fidelity
LoS	line of sight
LED	light-emitting diode
LIoT	light-based internet of things
MFTP	maximum flickering time period
MSM	metal-semiconductor-metal
M2M	machine to machine
MPPT	maximum power point tracking
MPP	maximum power point
MCU	microcontroller unit
MOSFET	metal–oxide–semiconductor field-effect transistor
NOMA	non-orthogonal multiple access
OOK	on off keying
OSC	organic semiconductor
OPV	organic photo voltaic
OFDM	orthogonal frequency-division multiplexing
PV	photovoltaic
PD	photo detector
PE	printed electronics
PCB	printed circuit board
PPM	pulse position modulation
PCE	power conversion efficiency
PET	polyethylene terephthalate
RF	radio frequency
R2R	roll to roll
RFID	radio-frequency identification

SPI	serial peripheral interface
SNR	signal to noise ratio
SL-APD	superlattice avalanche photo detector
SAF	set and forget
TTL	transistor to transistor logic
TFT	thin film transistor
TPC	transiently powered computers
UVLC	underwater visible light communication
URLLC	ultra-reliable low latency communications
VLC	visible light communication
WGPD	wave guide photo detector

1 INTRODUCTION

In present world, the concept of wireless technology is well established, and many technological applications are evolving based on it. As a consequence of that, the communication networks need to support increasingly large data traffic over shared radio frequency (RF) spectrum. Catering enough bandwidth for these requirements became a truly challenge for the current established technologies. Researchers forecast that, at end of the 2021 there will be about 1.5 mobile users' per capita rate with a total world base of 11.6 billion users. In addition, with the spectrum efficiency currently achievable, this number of users will be expected to demand approximately factor of 12000 more spectrum bandwidth compared to present capacity [1].This estimation creates a new problem, defined as "spectrum crunch", which describes the absence of frequencies in the remaining radio spectrum required to accommodate the exponentially growing number of mobile nodes [2]. Under these circumstances, with the evolution of 5G new radio technology, new communication technologies like enhanced mobile broadband (eMBB), enhanced machine type communications (eMTC), ultra-reliable low latency communications (URLLC) are expected to come alive. These technologies are promising to empower the machine to machine (M2M), device to device (D2D), device to everything (D2E) and internet of things (IoT) communications in 5G. However, accommodating a massive number of devices with these technologies within the existing spectrum will be challenging, and it re-emphasize the requirement of new unlicensed spectrum bandwidth [3]. As an alternative solution for this, optical communication which is, a relatively new wireless communication can be used. Recent studies suggest light fidelity (LiFi) spectrum as the best potential candidate for the new requirements. LiFi spectrum is made up with the combination of both visible light communication (VLC) and infrared (IR) spectrum. Moreover, the bandwidth of LiFi is approximately 2600 times larger compared to the whole radio frequency (RF) spectrum [4]. In addition, in [5] [6] authors have proposed non-orthogonal multiple access (NOMA) scheme for VLC systems which is well coincide with the promising multiple access scheme for the 5G technology. The above facts clearly suggest that the LiFi spectrum is a promising accommodator for the 5G and upcoming 6G technologies

Typical wireless nodes under 5G, for instance IoT nodes, come with unique challenges which will needed to be specially addressed. Since large number of connecting devices are required to deliver the desired outcomes of the IoT, limitations like energy consumption, battery life, cost per node and data rates need to be optimized accordingly [7]. Based on power availability and the expected operational lifetime, IoT devices can be mainly categorized under four types. Such as transiently powered computers (TPC), wearables, set and forget (SAF) and infrastructure and geophysical monitoring systems (IGMS) [8]. Researchers propose the use of renewable energy as a solution to the energy challenges. With this concept, IoT nodes are expected to self-generate/harvest their energy by using renewable energy and power up their energy optimized circuits. Ambient light, vibration motion, thermal energy and RF energy can be given as examples for the renewable energy sources. According to the researches, energy harvested from ambient light can achieve efficiencies in the range of 5-30% the largest compared to other approaches [9].

The cost and size per node can be minimized by using compact circuit design technologies such as printed electronics. Printed electronics is an emerging technology, which enables opportunity to manufacture cost-efficient compact electronics. The idea of this technology is to print circuit components and circuits using special materials which enable to manufacture them with currently existing large-scale printing technologies. This technology drastically reduces

the manufacturing time and cost while productions will be inexpensive so that they can be used in everyday life. In addition, printed electronics products can be made with flexible characteristics or can be moulded to fit in any form factor as desired [10].

1.1 Motivation

As discussed previously, moving the possible number of IoT applications to the VLC spectrum will support to reducing the current congestion in the RF spectrum. The characteristics of VLC enables to reuse same light wavelength between wall separated environment and it is free to use for everyone. This avoids the limitations to the IoT from the licensed spectrum bandwidth while accommodating massive number of IoT applications within the VLC spectrum. In the aspect of privacy and security, VLC creates a highly secure and private platform for IoT nodes to perform more secure data communication while eliminating the risk of eavesdropping from remote non-intend users. VLC can deliver data rates in large magnitudes up to the several Gbps [11]. Since most modern IoT applications require low to moderate data rates for its operations, these VLC data rates will be sufficient for the communication. In [12], authors purpose efficient coding technique - blinkcomm for the visible light-based IoT devices which enhance the data transmission rates. In addition, with the provided indoor illumination from VLC transmitters, indoor photo voltaic (PV) cells can harvest the energy needed by the IoT nodes [13]. To further make more compact the IoT physical design, printed electronics can be effectively used to optimally utilize the IoT node physical surface area. In addition, printed PV cells have the ability detect highspeed data signals while harvesting energy from the transmitter illumination [14]. Moreover, performance of the IoT nodes which made up with combination of both PV cell based energy harvesting and data receiving circuit can be further optimizable with the use of innovative data transmission schemes [15]. However, with the above discussed facts and recent findings support the importance of discover, study the feasibility and develop the proof of concept of the VLC based IoT node prototypes. This thesis will discuss important theoretical and practical information which we came across during the task

The goal of the thesis work is to prototype and implement an energy autonomous LIoT node. The device is expected to communicate using VLC while harvesting energy using printed solar cells and electronic circuitries. All supportive circuitry was selected based on commercial availability and they were chosen to support the final outcome of the node. However, as the PE technology is not yet fully mature, both PE and traditional electronics combination were used for the final implementation. The proposed model of prototype is illustrated in Figure 1.

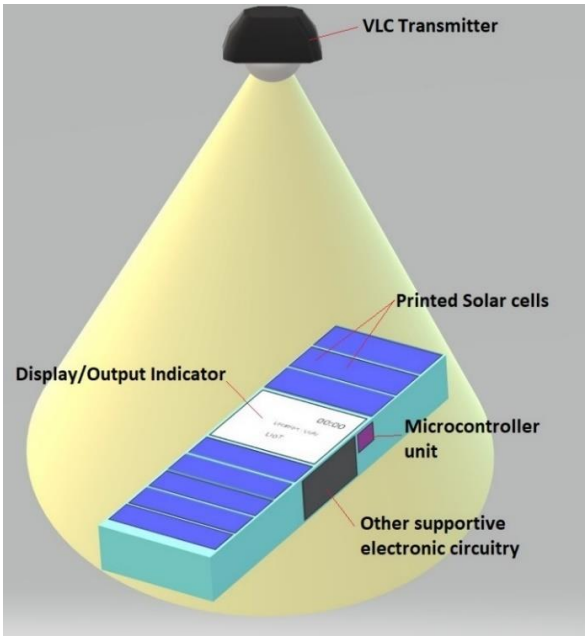

Figure 1. Proposed LIoT prototype model.

1.2 The goal of the work

The goal of this thesis is to study the practical feasibility of the Light-based IoT (LIoT) concept, where an energy autonomous IoT node is the key component [16]. The node exploits light to harvest energy and to communicate with an access point. The IoT node is based on the concept of "expose and connect" which follows the idea of communicating only when node is exposed to indoor illumination. In order to demonstrate the proof of concept of LIoT, an experimental prototype system was developed as a work of the thesis. Moreover, printed electronics-based components were used to demonstrate the effectiveness of printed electronic technology while making the prototype nodes more compact, low cost and large scale producible. The performance of the finalized prototype system was evaluated at the latter part of the thesis work.

The rest part of the thesis is organized as follows: In Chapter 2, an overview of VLC technology, theoretical background, channel characteristics and possible LIoT based applications are discussed. In Chapter 3, an overview of printed electronics and technologies are discussed. Chapter 4 presents the review and description of indoor energy harvesting unit. The Chapter 5 is reserved for design and implementation process of the IoT. In Chapter 6 the results and performance of the implementation are discussed. The discussion and the conclusions of the thesis work are described in Chapter 7 and Chapter 8.

2 OVERVIEW OF VLC CONCEPT, TECHNOLOGIES AND APPLICATIONS

2.1 Basic VLC concept

In VLC, the communication data is sent using visible light wavelengths which reside on the visible spectrum. The visible light spectrum spans between wavelength range of 380nm to 750nm corresponding to the frequency of 430 THz to 790 THz bandwidth within the LiFi spectrum [17]. The frequencies and their spectrum arrangement can be illustrated in Figure 2. The concept of VLC is to provide data communication via wavelengths visible to the human eye by utilizing the typical illumination infrastructure. The same infrastructure is used for both indoor lighting as well as data communications. LEDs can be modulated at high speeds, resulting in flicker-free operation suitable also for illumination purposes In IEEE 802.15.7 this technology is standardized as a candidate for wireless personal area networks [18].

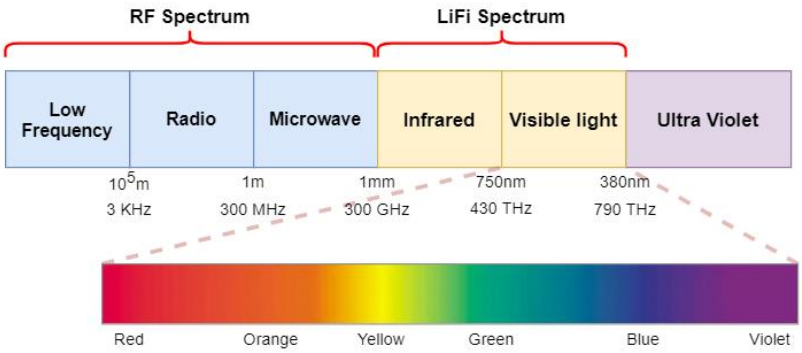

Figure 2. RF and LiFi Spectrum.

This chapter focuses on the basics and components of most common VLC system designs. The VLC system, transmitter, receiver and channel properties and their working principles are discussed respectively. The system architecture for VLC is depicted in Figure 3.

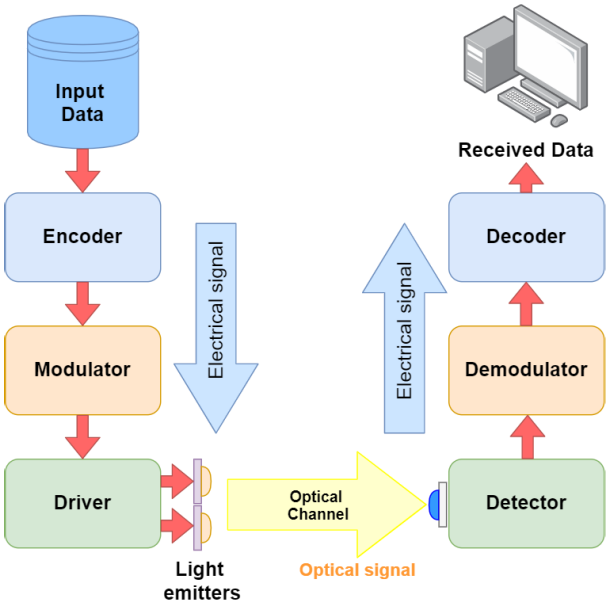

Figure 3. Common system architecture for VLC systems.

Initially, the data is encoded and modulated as mentioned earlier. Within the encoder and modulator, data bit streams are subjected to pre-equalization, in order to pre-compensate for any signal distortion that may take place in the optical channel. The data is coded and modulated in order to achieve higher throughput in the given bandwidth [19]. The modulated data signal is fed to the visible light emitter driver. Typically, LEDs are used as the light emitter at the transmitter. The driver makes the lights-based waveforms according to the modulation scheme used at the modulator. On the other end, the receiver transforms the received visible light waveform to an electrical waveform.

2.2 Transmitter

In a typical VLC system, the transmitter unit basically consists of encoder, modulator and drivers equipped with light emitters.

2.2.1 Light emitters.

In VLC transmitters, light emitters are used to create the visible light waves according to the modulated electrical signal waveform. As a result of recent research and development on lighting sources, LED light bulbs have become a strong candidate due to their low cost and compact VLC designs. Moreover, the compact, low power, small sized LEDs enable more opportunities to use VLC on various environment conditions [20]. In indoor VLC systems, the LED should be chosen to support for both data communication as well as indoor lightening purposes. Typically, wavelengths from 400 to 700nm are required to obtain resultant white light from the LEDs. Generally, for white indoor illumination, two types of LED bulbs can be used. These two types have their unique characteristics which can described as in Table 1.

Table 1. White LED types and characteristics

White LED Type	White light generating principle	Properties
Phosphor	Use blue light to excite the yellow phosphor and emit the white light	• Lower cost • Not support of complex modulation • Low response speed leads to lower modulation bandwidth
RGB (red, green and blue)	Built in with encapsulated red, green, blue LED chips to mix and produce resultant white light	• Complex modulation required • High response speed leads to support high data rates (through exploiting high-order modulation) • Higher cost

2.2.2 LED illumination and optical designs

The light distribution of LED tends to follow Lambertian distribution. However, according to the design requirement this light distribution can be modified. Optical lenses and reflectors can be used to vary the light pattern emitted by the LED. The Table 2 provides a summary of reflectors which can be used to LED lighting [21].

Table 2. Reflector designs and description

Style	Figures	Description
Direct		• LED light emitted directly without any optical arrangement. (Lambertian)
Diffusion		• Mostly used to reduce brightness while expanding light distribution range
Reflective	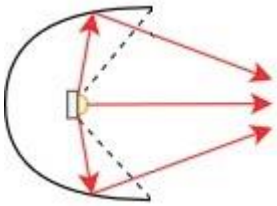	• According to this design, large angle light rays are get reflected by the reflector while central rays emit directly without reflections. • Different light patterns can be achieved by changing the reflector design
Transmission	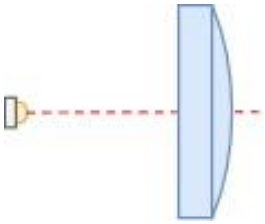	• The transparent lens can vary the intensity contours of the light distribution
Combined reflective and transmission	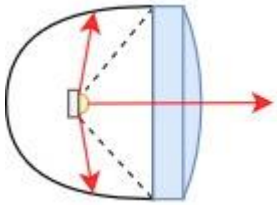	• This method contains both characteristics of reflective and transmission. • Varying the location of the lens, the number of reflections for large angle rays can be controlled.

2.2.3 LED Driver

In LED-based VLC transmitter, the LEDs will be controlled based on direct modulation techniques. Direct modulation techniques use drive current which contains a superimposed form of both direct current (DC) bias current and modulated data contain fluctuating current. The purpose of the LED driver is to control the light waves based on the receiving electrical signal. A summary of the direct modulation technique is illustrated in Figure 4.

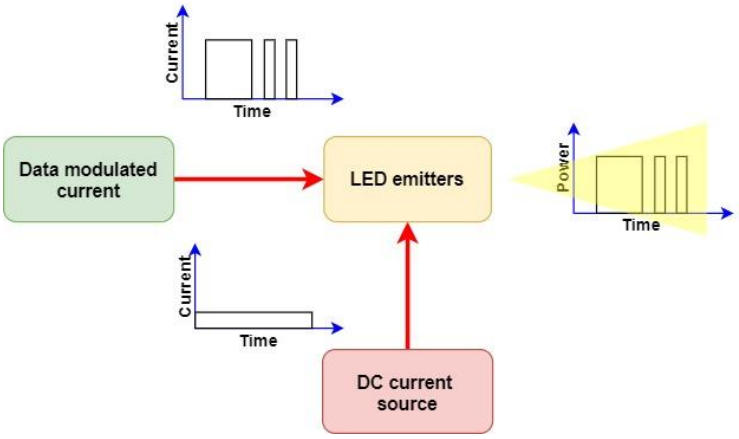

Figure 4. Structure of LED based direct modulation modulator.

The characteristic curve of LED is shown in Figure 5. According to the I-V curve of LED, voltage and current change approximately linearly when terminal voltage of the LED reached beyond V_{Active}. Therefore, LED driver should keep the transmitting LEDs in the linear operating region in order to provide efficient optical signal transition from the receiving electrical signal.

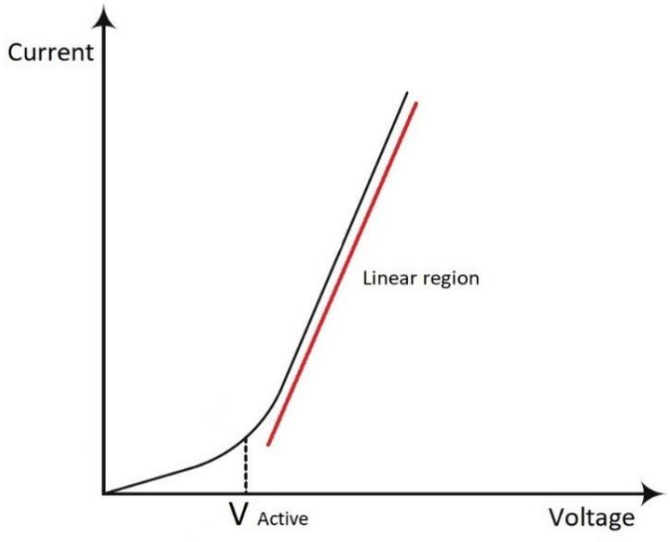

Figure 5. I-V curve of a LED.

The parameter of modulation depth can be defined as follows

$$m = \frac{\Delta I}{I_0}, \tag{1}$$

where, I_0 = bias current; ΔI = difference between peak and bias current.

Modulation depth describes the connection between modulated signal and DC bias given to the LED. Larger modulation depths make easier to receiver unit to detect optical signal. In addition, since modulation bandwidth defines the transmission rate and the VLC channel capacity in the system, it is important to design the driver circuit to achieve maximum modulation bandwidth. In LED based transmitter, maximum modulation bandwidth is limited by LED modulation bandwidth, which is defined on the construction material and geometry of the used LED type.

2.2.4 Modulation Schemes

In VLC systems, the used modulation schemes have direct impact on the transmission data rate. As a characteristic of commercially available LEDs, their half power (3dB) modulation bandwidth is about few MHz in size. The 3dB modulation bandwidth explains the LED's supported frequency range, which results more than half power of receiving at the receiver. Modulation bandwidth of given type of LED can be determined by the below equation

$$f_{3dB} = \frac{\sqrt{3}}{2\pi\tau_c}, \tag{2}$$

where; τ_c = lifetime of the minority carriers in the semiconductor

The issue of low modulation bandwidth can be overcome by improving the drive circuit design with high performance electronics. In addition, this can further enhanced by selecting the proper modulation scheme accordingly [22]

In order provide user friendly communication experience, the IEEE 802.15.7 standard mainly focuses on two aspects, as follows

- flicker mitigation
- dimming support

Flickering can occur as a result of LED low/off period during low rate data transmission which is noticeable to human eye and it can cause eye strain for the users. To mitigate flicker, variation/fluctuation of LED should take place within the maximum flickering time period (MFTP). MFTP express the maximum time period which is unnoticed to human eye and during that period light intensity should be changed. MFTP can be approximated as time frame below 5 milliseconds [23].

The dimming support explains the VLC system's ability of perform under the user-selected arbitrary light dimming conditions. According to that, VLC systems are expected to perform robustly even the indoor light intensity varies.

Few VLC compatible modulation schemes are described on Table 3. [24]

Table 3. VLC modulation schemes comparison

Modulation scheme	**Description**
On off keying (OOK)	High voltage level used for bit 1 while zero voltage level used for 0 bit in binary representation
Colour shift keying (CSK)	Transmits data based on red, green, and blue lights. Power level of the resultant waveform is constant
Pulse position modulation (PPM)	Same voltage level is used for both binary bits while their pulse duration will be adjusted to separate the bits
Orthogonal frequency-division multiplexing (OFDM)	Orthogonal frequencies will be used to transmit parallel data streams

2.3 Receiver

2.3.1 Detector unit

In VLC systems, the purpose of the detector unit is to detect the visible light waveform and transform it into an electrical waveform. There are several characteristics expected from detector devices. High responsivity within the desired wavelength or spectrum is expected in order to get high quality electrical waveforms from the incident optical waveforms. In addition, fast response speed is crucial for high speed broadband VLC systems. To minimize the distortion, the detector unit should be able to maintain low noise levels when converting optical signal to electrical signal. Moreover, the relationship between optical – electrical domains is expected to be a linear, to get better performance.

- Photo detectors (PD): PDs are designed to detect optical signals with wider spectral response. Most commonly available PDs are positive-intrinsic-negative (PIN), avalanche PD (APD), metal-semiconductor-metal (MSM-PD), Single photon avalanche diode (SPAD), superlattice avalanche (SL-APD), wave guide PDs (WGPD) and cavity enhanced photoelectric PDs (RCE – PD) etc. When the PD is exposed to an optical signal, the PN junction within the PD starts to produce the electrical current linearly proportional to the optical signal

- Photovoltaic detectors: Solar panels can be used as visible light detectors.

2.3.2 Receiver circuit

A typical structure of photodiode-based receiver is illustrated in Figure 6. Initially, the photodiode receives optical signal through the channel and converts it into time varying current signal. The transimpedance amplifier converts current signal into voltage waveform so it can be modified using conventional methods. Then, the signal is filtered in order to remove noise components within the signal. In indoor conditions, most of noise components are generated due to ambient sunlight and other indoor luminaries which are typically operated around low frequency from the power line. Frequency tuned bandpass or high pass filters can be used for this purpose. In [25], authors have purposed a Sallen-key high pass filter circuit arrangement for VLC receivers. However, researchers have found several other alternative ways to mitigate

noise components from the signal. According to [26], an adaptive minimum voltage cancellation circuit can be used to mitigate noise effects by adaptively subtracting the minimum voltage from the waveform. Moreover, in [27] authors have proposed use of Schmitt-trigger comparator arrangement in order to precisely detect the signal waveform and get rid of the low noise components for VLC receivers. Thereafter, the noise-removed signal is amplified through the automatic gain-controlled amplifier. The amplified signal then gets post-equalized. There are several post- equalization methods to re-correct the distorted received waveforms. Post-equalization methods can be divided into two main groups, namely frequency domain and time domain approaches [28]. Finally, the signal waveform gets demodulated and decoded according to the configurations.

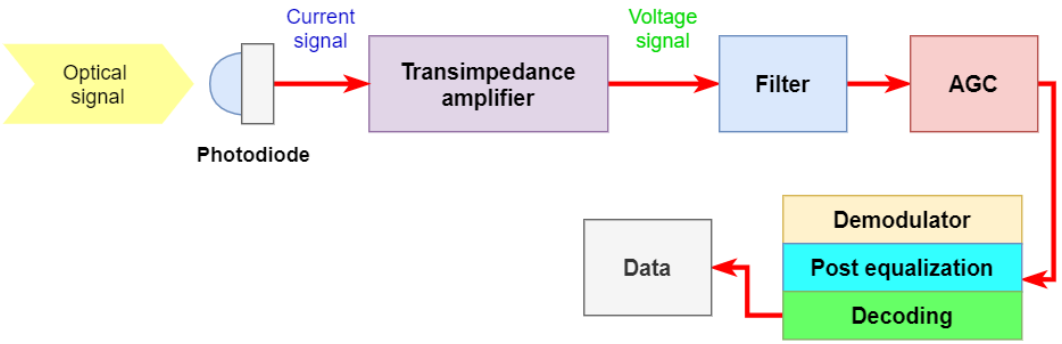

Figure 6. Structure of a PD based receiver.

2.4 VLC Channel Characteristics

In a VLC system, the transmission model can be expressed as

$$Y(t) = RX(t) \otimes h(t) + N(t), \tag{4}$$

where Y(t) = received signal; X(t)= power of transmitted light, h(t) impulse response of the channel N(t) = additive white Gaussian noise and R = photodiode's photoelectric transformation efficiency.

The summary of transmission model is illustrated as Figure 7.

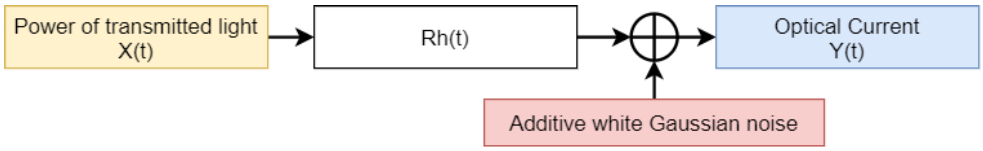

Figure 7. Linear baseband transmission model of an indoor VLC.

According to [29], VLC links can be divided as directional and non-directional. The categorization is based on the angle of transmitting and receiving beams. Beam will become

nearly parallel if the divergent angle is small in the transmitter's end. From the receiver's point of view, if the angular view of the photodiode unit is small, the ability of receiving will be limited to towards one direction. Therefore, it called as a directional receiver. A detailed illustration of a directional link is given in Figure 8a. In the case of both transmitter and receiver are directional, the link is set up in a way that both units are aligned to each other. However, if both transmitters and receivers have large transmitting and receiving angles, the link is called non directional link. There is a type of link that made up with mix of these two types of transmitters and receivers which is called as a hybrid links. Illustrations of non-directional and hybrid links are given in Figure 8b and Figure 8c.

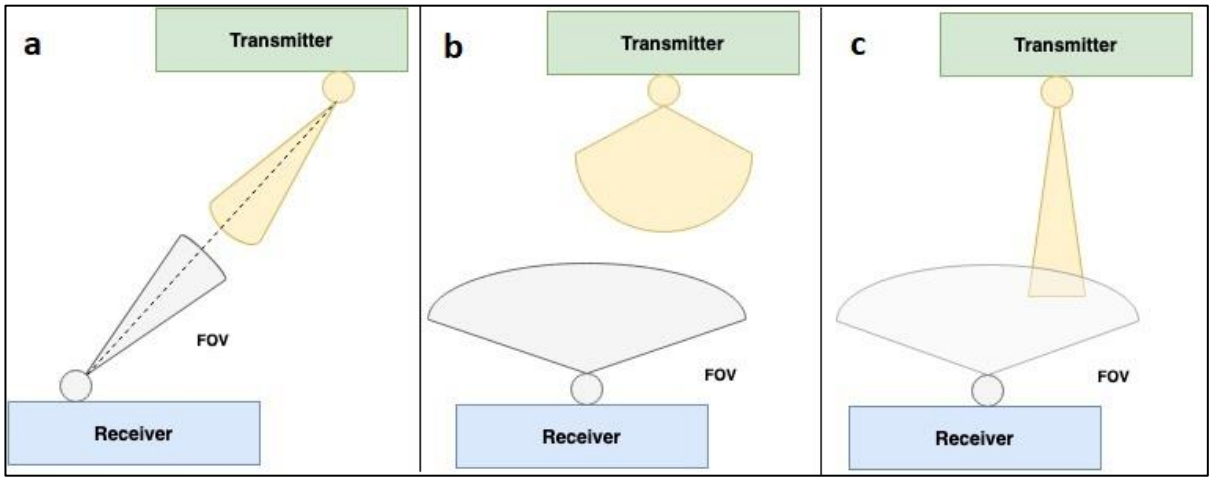

Figure 8. Directional (a), non-directional (b) and hybrid (c) link types.

Furthermore, VLC links can be also categorized as line of sight (LoS) and diffuse links. Similar to other communication channel models, LoS link describes the direct aligned communication link between transmitter and receiver which utilizes the high-power transmission. Diffuse links are useful when scenarios like shadowing phenomena, which reduces the strength of LoS link [30]. It is important to design transmitters and receivers with less directional requirements in order to maximize the use from diffuse links. The structure and parameters of these types of links are given in Figure 9.

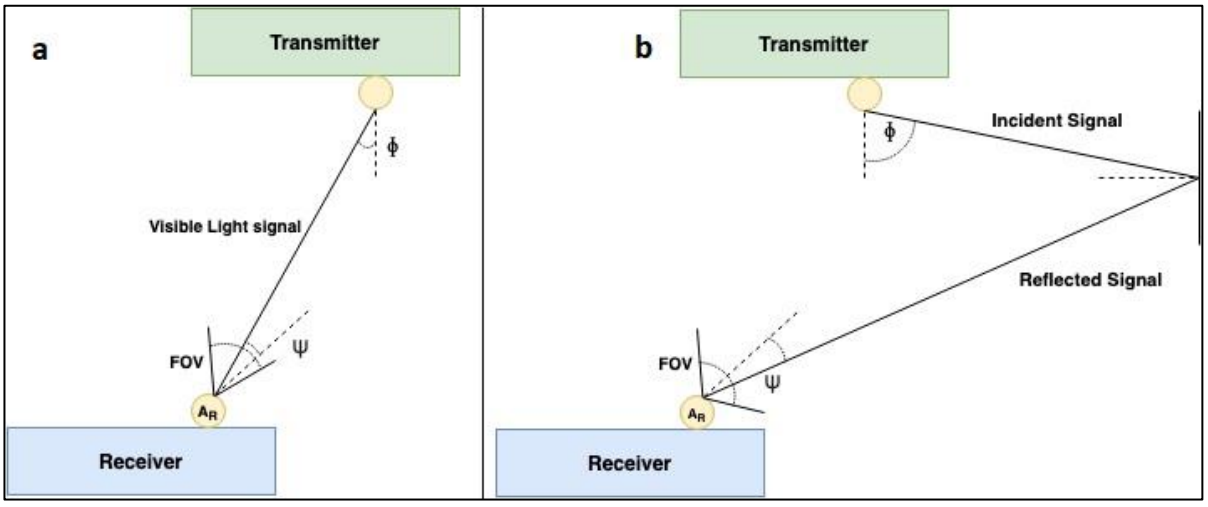

Figure 9. LoS (a) and diffuse (b) links.

2.4.1 VLC channel model

In VLC system, the channel model can be expressed as follows

$$H(f) = \sum_i H_{LOS,}\, ie^{(-j2\pi f \Delta\tau_{LOS,i})} + H_{diff}\, \frac{e^{(-j2\pi f \Delta\tau_{diff})}}{1+jf/f_{cutoff}}, \quad (5)$$

where; $H_{LOS,i}$ = channel gain of i^{th} LoS components; H_{diff} = diffuse signal gain $\Delta\tau_{LOS,i}$ = delay of i^{th} LOS components; $\Delta\tau_{diff}$ = delay of diffuse signal components and f_{cutoff} = cut-off frequency of diffuse channel frequency response.

2.4.2 LOS components

In LED driven VLC system, the LoS gain from the i^{th} white LED can be obtained by following expression

$$H_{LOS,i} = \frac{A_R(m+1)}{(2\pi r_i^2)}\, cos^m(\phi_i) t_s(\psi_i) g(\psi_i) \cos(\psi_i), \quad (6)$$

where; A_R = Active area; ϕ_i = transmit angle w:r:t maximum radiation direction of the i^{th} light source; ψ_i = angle of irradiance; r_i = distance to the illuminated surface ; $t_s(\psi_i)$ = transmission of optical filter and $g(\psi_i)$ = gain of non-imaging concentrator.

2.4.3 Impulse response

The Impulse response of i^{th} LoS component can be obtained from follow equation

$$h_{LOS,i}(t) = \frac{A_R(m+1)}{(2\pi r_i^2)}\, cos^m(\phi_i) t_s(\psi_i) g(\psi_i) \cos(\psi_i) \delta(t - \frac{r_i}{c}). \quad (7)$$

2.4.4 Diffuse components

Diffuse gain can be obtained from following. In most cases this is modelled as a constant

$$H_{diff} = \frac{A_R\, r_{refl}}{A_{Room}\,(1-r_{refl})}, \quad (8)$$

where; A_{Room} = room area; r_{refl} = average reflectivity.

2.4.5 The luminous flux

The line of sight gain provide from i^{th} light source is subjected to the luminous flux. The luminous flux can be expressed as

$$\Phi = K_{max} \int_{380\,nm}^{780\,nm} \Phi_e(\lambda)\, V(\lambda)\, d\lambda, \quad (9)$$

where; $\Phi_e(\lambda)$ – source power distributions; $V(\lambda)$ – standard sensitivity function and K_{max} – source power distributions.

2.4.6 Radiation intensity

In VLC environment, the radiation intensity at given point can be obtained by

$$I(\phi) = I(\phi = 0)\,(\cos(\phi))^m, \tag{10}$$

where; $\phi =$ transmit angle with respect to maximum radiation direction and m represents the Lambert index corresponding to the VLC source radiation semi angle, which can be expressed as

Lambert index = -1/$log_2(cos\theta_{1/2})$ and $\theta_{1/2}$ = Source semi angle at half power.

2.5 VLC system performance

In VLC system, signal quality of the received signal can be evaluated by calculating the signal to noise ratio. The signal power can be expressed as

$$S = \gamma^2 P^2_{received\ signal}, \tag{11}$$

where;
$$P_{received\ signal} = \int_0^T [h(t) \otimes X(t)]dt. \tag{12}$$

The noise is considered as a summation of thermal, shot and inter-symbol interference

$$N = \sigma^2_{thermal} + \sigma^2_{shot} + \gamma^2 P^2_{received\ ISI}, \tag{13}$$

where;
$$P_{received\ ISI} = \int_T^\infty [h(t) \otimes X(t)]dt. \tag{14}$$

2.5.1 Thermal noise

In VLC systems, thermal noise component is caused by the random thermal motion of electrons in the load resistance. This phenomenon also called as Johnson noise. In photodiode-based VLC receivers, thermal noise can occur in transimpedance amplifier stage which use multiple load resistance to convert photocurrent to voltage signal. [31]

The thermal noise power spectral density is defined as

$$\mathrm{S_{thermal}} = \frac{4k_BT}{R_L}, \tag{15}$$

and thermal noise power is defined as

$$\mathrm{P_{thermal}} = \frac{4k_BT}{R_L}\,\Delta f. \tag{16}$$

The variance of the thermal noise can be given by

$$\sigma_{thermal}^2 = \frac{8\pi kT}{G}\eta A I_2 B^2 + \frac{16\pi^2 kT\Gamma}{g_m}\eta^2 A^2 I_3 B^3, \quad (17)$$

where; T = absolute temperature; k_B = Boltzmann's constant ; Δf = receiver bandwidth G = Open loop gain and I_2 = noise bandwidth factor.

2.5.2 Quantum shot noise

In photodiode-based VLC receivers, shot noise is a component which caused by the dark current fluctuations. This phenomenon occurs due to randomly produced currents in different areas of the photodiode surface.

The variance of the shot noise can be given by

$$\sigma_{shot}^2 = 2q\gamma\left(P_{rSignal} + P_{rISI}\right)B + 2qI_{bg}I_2 B, \quad (18)$$

where; q is the electron energy, B = noise bandwidth and I_{bg} = background current.

2.6 LIoT Concept: Possible Applications

2.6.1 IoT based Product label

By exploiting the idea of printed electronics and LIoT, the labels of future products can be designed to be active. VLC transmitters can be integrated to the lighting infrastructure of the shop while integrating the receivers with printed compact PV cells in the label. In this way, multiple batches of same product can be updated simultaneously. Further, this method provides opportunity to use same transmitter infrastructure for any of compatible products. The transmitted data is expected to be displayed on the flexible display integrated in the label which made by printed electronic technology. Using this method, product prices, special notes such as seasonal greetings, sale banners can be dynamically updated according to the seller's/manufacturer's requirements. In addition, by adding circuitry for checking product quality, such as tiny sensors for detecting density changes or colour changes in contained liquids, the approximated expiry date of the product can be accurately predicted. Such methods can help to correct the changes of expiry date due to erroneous conditions during product storage. The display units need to be chosen with low energy consumption and multistage stable displays so that whenever the product is taken out from the shelves label will freeze. Also, by adding situation-aware animated brand name logos, mini animations or dynamic text, the aesthetical appearance will be enhanced while creating new platform for creative advertisement, logistical use, etc. This concept is illustrated in Figure 10.

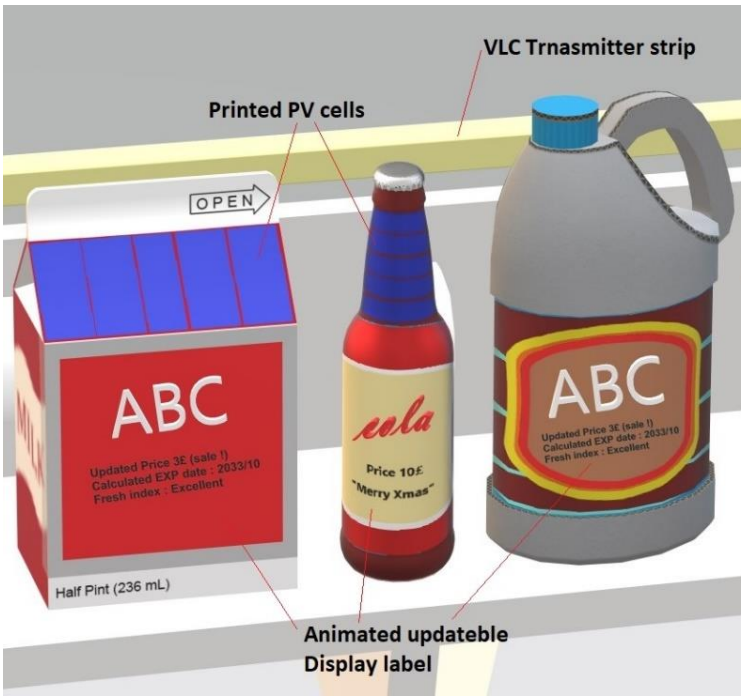

Figure 10. Concept of LIoT based product label.

2.6.2 LIoT based wireless communication device

The concept of energy autonomous LIoT can be applied to daily communication applications. Devices such as museum audio guides, conference translators, indoor audio headphones and similar devices can be further simplified using this concept. Since the devices are expected to be energy autonomous, new devices will not need battery which will lead to more compact and lifetime durable designs. This will make users to simply forget about the battery charging intervals while providing limitless audio user experience. Another advantage is this technology makes these devices completely hazardless due to zero energy storage nature. Typically, batteries are considered as fire hazardous energy storing device which should be stored and transported under defined regulations. In addition, VLC has proven to support higher data rates compared to Bluetooth technology, which is widely used in wireless audio devices [32]. This provides the opportunity to use higher quality audio transmission with higher audio rate, which will enhance user experience. Moreover, by establishing a common VLC platform in public places such as museums, trains, conference halls create opportunity to people to use their own wireless audio devices without borrowing specifically designed devices for each place. This concept can be further enhanced by adding uplink such as IR or RF so that this can be applied in all duplex devices currently existing. This concept using scenario is illustrated in Figure 11.

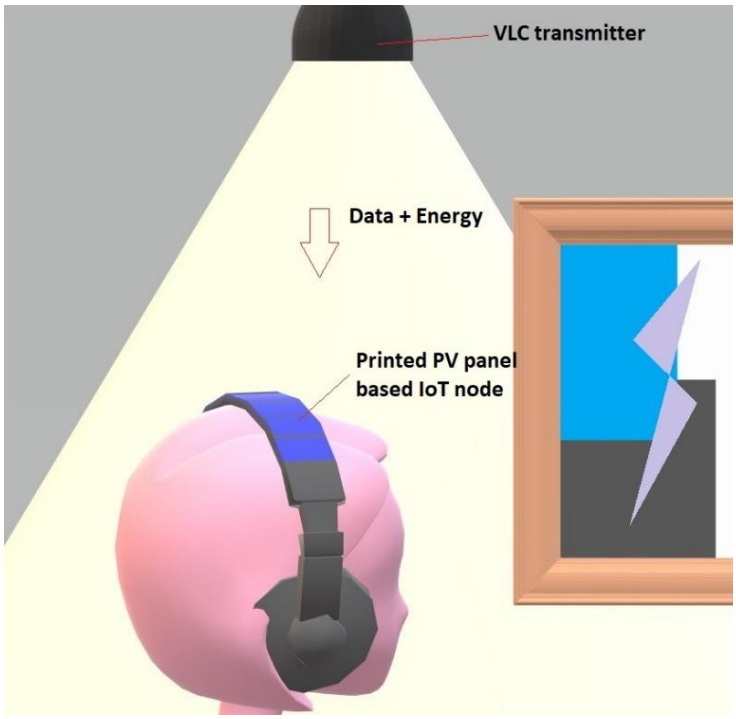

Figure 11. Concept of LIoT wireless communication devices.

2.6.3 LIoT - based shallow underwater wireless IoT

The self-energy harvesting VLC based IoT concept can enhance the underwater communication experience. VLC is promising to give faster Gbps underwater data rates, which goes way beyond the kbps data rates of acoustic signals currently offering to the underwater devices [33], [34]. According to [35], there are multiple modulation schemes available which can be used for Gbps scale data rate underwater VLC (UVLC). In [36] authors describe underwater-capable efficient PV cell design which can be used for energy harvesting. The LIoT concept can be easily used to shallow water communication equipment applications, small scale drones as well as IoT sensors submerged in the transparent liquids. As advantages, the LIoT nodes will not need to be maintained on regular interval and moreover, the less complex concept will help making more robust, inexpensive underwater communication devices for commercial use. A practical scenario of utilizing this concept is illustrated in Figure 12.

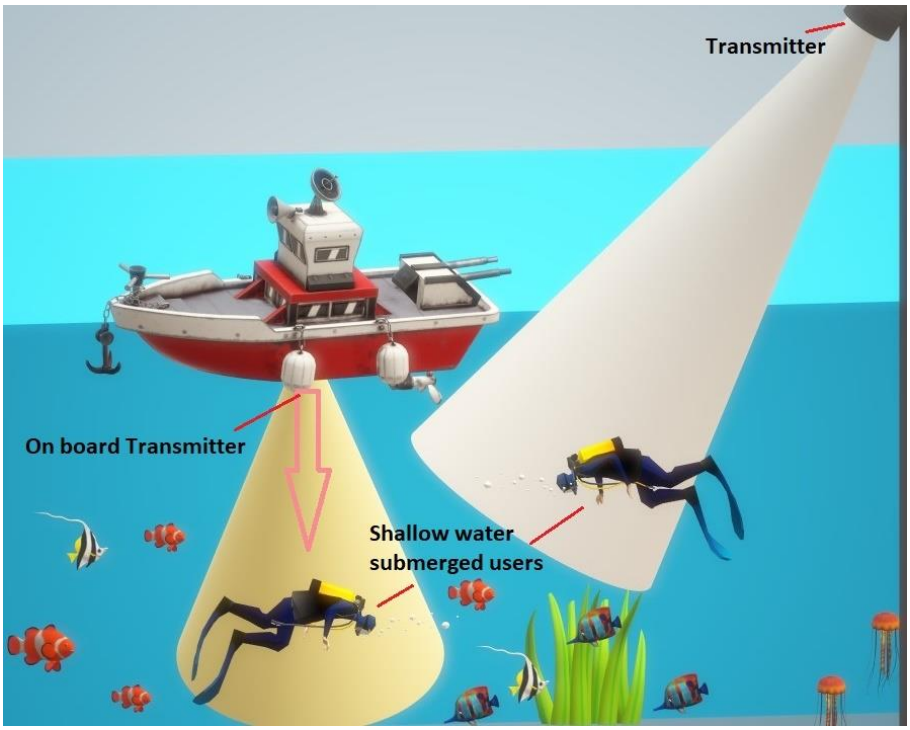

Figure 12. Concept of LIoT based shallow underwater wireless IoT.

2.6.4 LIoT based indoor position systems

This concept can be effectively used for indoor position locating applications. Since, light-emitting diode (LED) lighting is rapidly becoming more popular for indoor illumination, this LIoT based positioning concept can be implemented on existing illuminating infrastructure effortlessly. In this application, the user node is expected to receive the location coordinates from closest VLC transmitter luminary and based on that user's location will be dynamically updated. The location mapping devices can be designed by using microcontrollers and bistable displays like electrochromic or e-ink such that hold the previous state in case of no new data is received. Printed solar cells can be placed on the surface of the device. As illustrated in Figure 13, the locating device can be made more compact, energy autonomous, and more importantly, inexpensive in order to make them feasible for any scale service providers. The locating devices are expected to preserve the conventional style of maps which is simple and more familiar with generations of users. These indoor positioning systems can be used in places like supermarkets, universities, libraries and shopping malls in order to help customers to locate their items quickly. In addition, this concept will be useful to customers to overcome language barriers and have a better shopping experience.

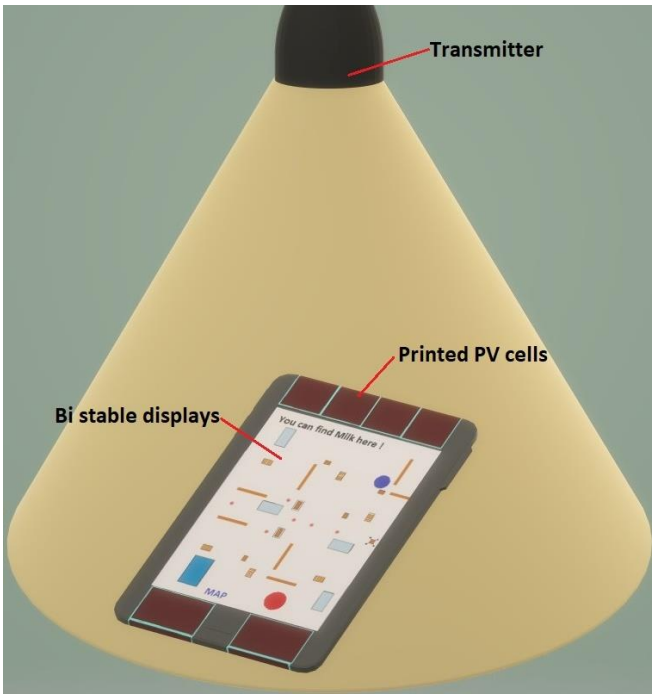

Figure 13. Concept of LIoT based indoor position systems.

3 INTRODUCTION TO PRINTABLE ELECTRONICS

The sudden surge of demand for small electronic devices can be attributed to the IoT concept, that emerged from 5G. Device manufacturers lean towards new materials to make compact and cost-efficient designs. The rigidness of existing silicon-based printed circuit boards (PCB) are limiting the designer's ability of making small designs up to some extent. As a promising solution for this, printable electronics is rapidly becoming a key implementation technology due to its unique features compared to the traditional PCB electronics. This technology has the ability to produce electronic circuitries on flexible substrates and materials which are mechanically flexible or stretchable without any damages to the design [37]. In addition, less complex process of manufacture enables personalized fabrication of circuits for the designers. This utilizes the maximum space in the device while making it smaller and compact. This advantage considered as a key feature of this technology. Designing of printable electronics can be done following two approaches [38].

1. Component type: This type focuses on designing flexible electronic components such as resistors, capacitors and transistors based on organic or inorganic semiconductors.

2. System type: These types of designs are focused on designing complete circuitries using printed electronic techniques. The productions are expected to be work as traditional rigid circuits while preserving unique flexible, stretchable characteristics.

The main concept of printed electronics was emphasized with the invention of electronic ink. When fabricating printed electronics, electronic inks is deposited on the flexible substrate. An illustration of inkjet-based ink deposition is given in Figure 14. As illustrated in Figure 15, after depositing the ink, the substrate with ink is annealed or sintered to bring back the characteristic properties of ink [39].

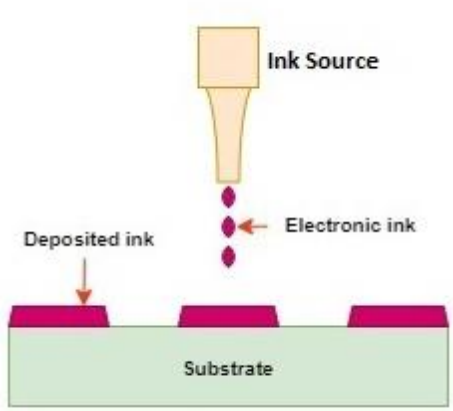

Figure 14. Ink deposition.

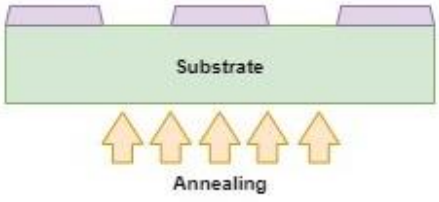

Figure 15. Sintering and annealing process [37].

3.1 Electronic Ink.

The electronic ink consists of functional material, stabilizers and rheological modifiers. The purpose of functional materials is to provide expected characteristics to the printed element. For dielectric elements, functional material will be chosen based on the insulating characteristics while, conducting characteristics will be considered for the printed electrode elements. Stabilizers and the rheological modifiers will be selected based on application and the method of fabrication. These materials must have good stability and ability to withstand long lifetime under the conditions subjected to the nature of application while they should be inexpensive and environment friendly [40].

Electronic inks can be basically categorized as organic and inorganic. Most of early days electronic inks were based on organic materials. These organic materials are available as water soluble large molecular compounds (polymers), which can effortlessly convert to liquid ink. However, conductive properties of these polymer organic materials are found to be much smaller compared to the small molecular organic materials. In order to create flexible electronics, molecular organic inks can be deposited on the flexible substrate by using printing or vacuum evaporation ink deposition methods. [41]

On the other hand, inorganic materials are rapidly evolving, having advantages over the organic materials. Inorganic material-based inks are promising to give better conductive performance and good environmental stability whereas printed organic materials tend to degrade when they contacted with oxygen and humidity over the time. Inorganic materials can be turned to electronic ink by dissolving the solid-state powder of inorganic compounds in solvents. After printing the elements or circuit using inorganic ink on the substrate, sintering process need to be done.

The sintering process re-transforms the inorganic material components in the printed ink back to solid state, enabling the most solid-state properties of inorganic material again. Since sintering process requires higher temperatures, suitable substrates were limited, and they needed to be selected to withstand the high temperature conditions. As a remedy for this, inorganic nano materials were introduced. Nano materials only required sintering temperature below 150^0C and it aided the use of thin films substrates materials [42]. Examples for inorganic materials based electronic inks are given in Table 4.

Table 4. Types of functional ink and examples

Type of functional ink	**Examples**
Conductors	nano silver, nano copper, ITO
Semiconductors	single-walled carbon nanotube, metal oxide

3.2 Substrates for printed electronics

In PE, the mechanical characteristics of the circuit majorly depend on the properties of the substrate. There are three types of substrates can be used in PE. They are glass, metals and polymers. For the flexible devices, metal and polymers would be the ideal candidates due to their mechanical flexibility. However due to the large design cost and constrained design freedom on metallic substrates, non-reinforced polymers are vastly used as substrates for the flexible devices. The major drawback of non-reinforced polymers is their low surface energy. Surface energy describes the ability of attracting other depositing material's molecules into the substrate surface. To increase the surface energy, prior surface treatments are used. When

selecting substrate for an application, properties of mechanical, physical, chemical and thermal aspects are needed to take to the consideration. Various types of flexible substrates listed on Table 5. The extensible substrate materials have the ability of stretching without damaging the circuits while flexible substrates have the ability of mechanically bending without damaging the circuits.

Table 5: Types of flexible and extensible substrates.

Flexible substrates	**Extensible substrates**
polyimide	polyurethane
polyethylene terephthalate	thermoplastic polyurethanes
polyethylene naphtholate	

3.3 Printing flexible electronics

In this section, the manufacturing process of typical printed electronics components will be described.

*3.3.1 **Component type electronics**.*

As discussed in the introduction chapter, printing electronic components such as transistors, resistors and capacitors with flexible characteristics are vital to make compact flexible also low-cost circuitries. Among those, transistors can be used as the main building block to create more advanced circuits. To create printed transistors on flexible substrate, thin film transistor (TFT) structure can be used. The structure of TFT is illustrated in Figure 16.

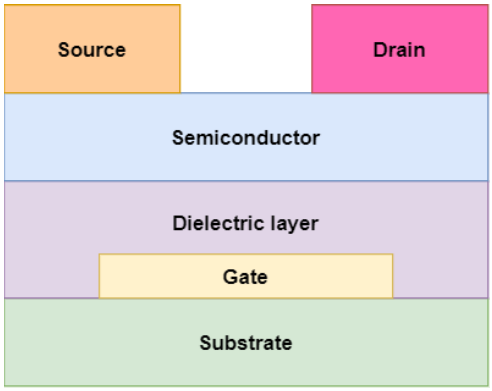

Figure 16. TFT structure.

There are several types of TFTs, such as phousilicon, polysilicon metal oxide and organic TFTs. In order to manufacture TFTs on substrate, annealing process needed to be done. Annealing is a process which heats up hard metals in order to get soft malleable metal for the manufacturing process. Due to its low annealing temperature, organic TFTs can be manufactured by printed techniques on flexible substrates [43]. The TFTs printed with inorganic inks such as semiconducting single-walled carbon nanotube inks are considered as transistors with high performance characteristics on conductivity, physical flexibility and environmental stability.

3.3.2 System type electronics

With use of large printed electronic components, a complete electronic circuit can be completed. The connections between components are printed using flexible or stretchable conducting inks on flexible substrates. In addition, flexible circuits can be made with commercially available rigid electronic components. These type designs are called as flexible hybrid electronics (FHE). These circuitries are produced by placing of conventional rigid components on flexible/stretchable substrates so that final design has the mechanical characteristics of printed electronics and involvedness of traditional electronics. This will permit the printed electronics system to evolve, despite of slowly developing printed component electronics. To make flexible conductive connection in-between the components, nano silver ink is commonly used. The low sintering temperature of nano inks enables the use of polyethylene terephthalate (PET), paper substrates which have excellent flexibility and cheap printing costs.

3.4 Printed electronic fabrication method classifications

There are several methods to manufacture printed electronics. Based on the direction of fabricating, these methods can be categorized into two main types as follows

1. Top – down technologies
2. Bottom – up technologies

3.4.1 Top – Down technologies

These technologies follow the main idea of depositing and pile up electronic ink on the flexible/stretchable substrate. Few examples of top down technologies are listed next.

1. Dip pen
2. Screen printing
3. Ink jet
4. Offset printing

The main advantage of top-down technologies is that, their printing mechanisms are compatible with large scale production methods, such as roll to roll production. These printing methods result in low cost per unit at faster production time. As a disadvantage, the top deposition method some time does not create strong bond between the functional ink compared to bottom-up technology.

3.4.2 Bottom – up technologies

Instead of depositing ink from top of the substrate, these technologies take different approaches. The basic approach is to use chemical reactions for produce functional materials on the substrate.

Examples for bottom up technologies

1. Polymer-Assisted-Deposition
2. Ion-Exchange Technology

The main advantage of these technologies is that, they create strong bonds between the functional material and the substrate which make more robust designs for some applications. Moreover, in [44], authors have classified the printing methods as following

- Contacting printing (Dip pen, Screen, Offset)
- Non-contact printing (Ink jet, Laser directed)

This classification is based on whether the substrate is going not that clear or not when depositing the ink.

3.5 Manufacturing methods for large scale PE productions.

3.5.1 Roll-to-Roll Technology (R2R)

To increase the throughput, manufacturers are using "roll-to-roll" technologies inspired from these concepts. The concept of R2R printing can be explained from below Figure 17. It depicts the design sequence of TFT described in Figure 16. Each layer corresponding to the TFT structure is deposited one by one using connected sequence of printers. The production starts from a roll of thin undeposited substrate and then the printer system begins to deposit the E-ink on the substrate. After the completion of ink deposition on the substrate, the final output substrate is stored in a roller.

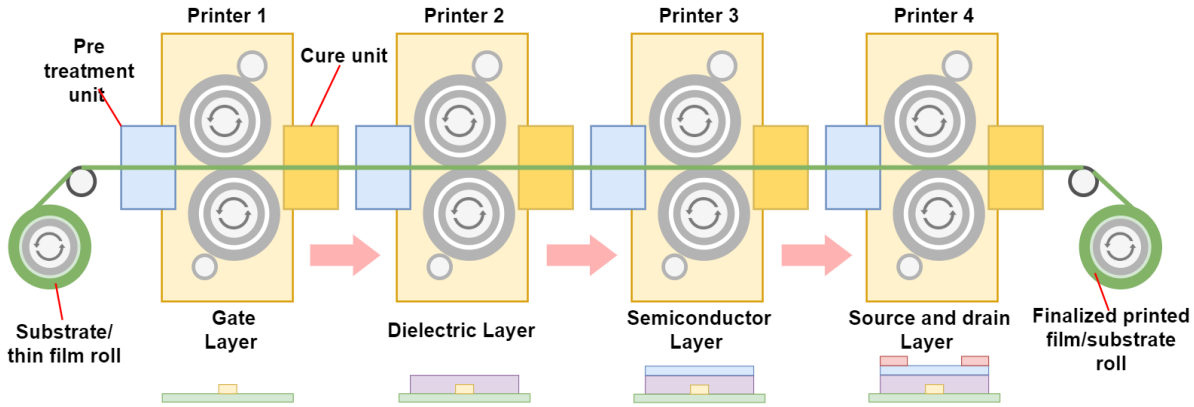

Figure 17. Roll-to-roll printing method (R2R).

3.5.2 Dip – Pen technology

In this method, ink molecules which deposited on atomic force microscope are transferred to the surface of the substrate. The tip needed to be contacted on the substrate in order to transfer the ink. The low required annealing/sintering temperature in this technology enables printing on more spectrum of compatible substrates. Figure 18 illustrates the e-ink deposition on substrate using atomic force microscopic tip.

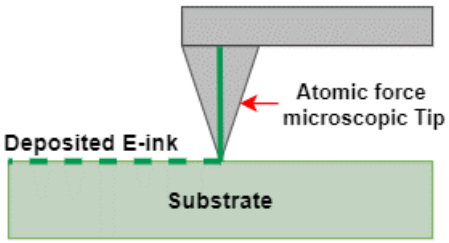

Figure 18. Dip-pen ink deposition.

3.5.3 Screen printing technology

To manufacture screen printed circuit using screen printing, basically five components are required. They are, stencil according to the circuit or component, a squeegee, functional ink, a screen printer stage and a substrate. Figure 19 illustrates the screen-printing process using these items. In this technology, the functional ink is deposited on the substrate by using a stencil and squeegee. In this method, the viscosity of electronic ink and the squeegee quality play vital roles respect to the connection between the ink and substrate. The major advantage of screen printing is its ability of depositing printed image with great thickness on the substrate. The thickness of the image is subjected to the thickness of used stencil and the deposited ink can be thick as more than 100µm, which is an unique ability to this technology [45]. Moreover, due to simple procedure and great feasibility for large scale production, this technology became as one of most popular methods in the PE industry.

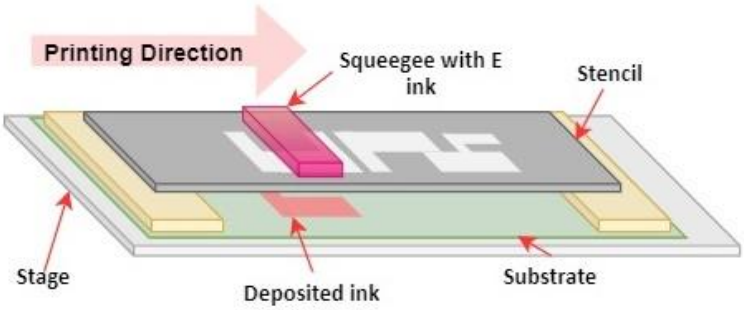

Figure 19. Screen printing method.

However, compared to other methods, screen printing is relatively a slow printing technology due to its printing mechanism. To overcome this, the rotary screen-printing method is used in mass scale production. This printing mechanism is illustrated in Figure 20. In this method, stencil and squeegee mechanism integrated in a roller in order to maximize the throughput of the production.

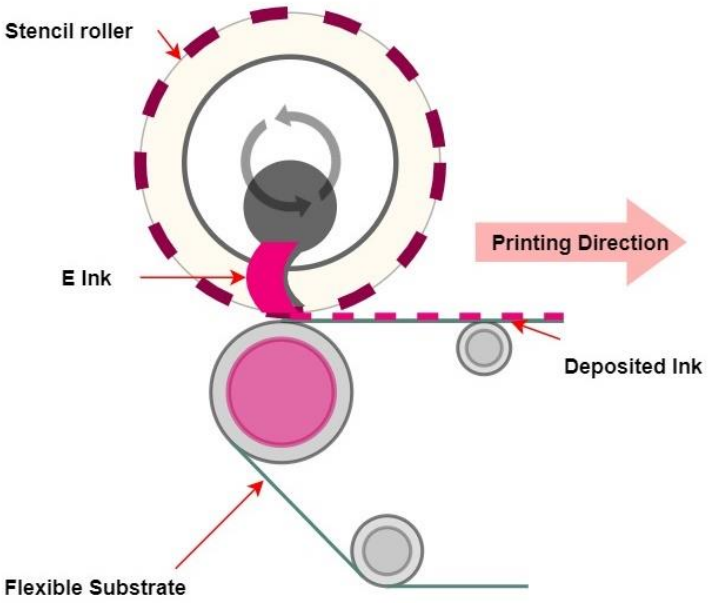

Figure 20. Rotary screen printing.

3.5.4 Inkjet technology

Inkjet is a top down PE fabrication technology similar to the concept of day to day office inkjet printers. This method enables direct writing on the substrate without being limited to any direction constrains while facilitating effortless ink deposition on any arbitrary shaped substrates. Figure 21 describes the ink deposition process of this method. There are two main types inkjet technologies available.

- Continuous inkjet (CIJ).
- Drop on demand mode (DoD).

In this CIJ technique, piezoelectric transducers in the printing nozzles release functional ink droplets to the substrate based on the design oriented electronic signal. There are four types piezoelectric nozzles available. They are grouped as squeeze, shear, bend and push. Each of these types has a particular droplet feature. Moreover, in this technology, the parameters such as piezo voltage, droplet weight and printing speed are directly determining the quality of the printed design on the substrate.

In DoD method, parallel ink nozzles are used, and they are only activated when needed. Pulses based signal is used and at each pulse nozzles are configured to release droplets. This printing method is low cost relatively compared to CIJ method [46]. Ink jet technology vastly used for PE applications like transistors, flexible sensors etc.

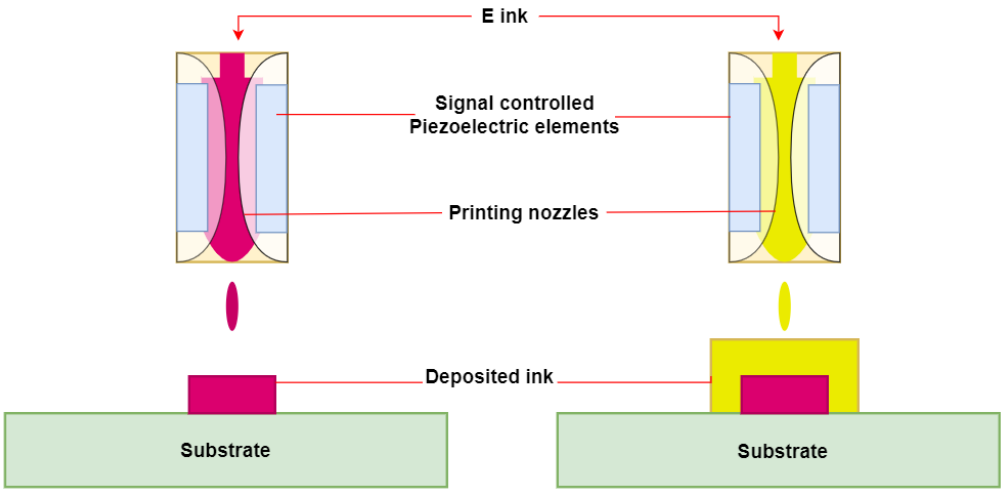

Figure 21. Inkjet ink deposition method.

3.5.5 Offset-Gravure Printing

This offset printing method is popular for its high-speed printing ability compared to other methods. In this method, initially, the design is placed on the gravure plate. then the plate rolled over the gravure roller. Thereafter, functional ink is soaked over the gravure roll and doctor blade used to limit the available ink on the roll. Doctor blade is an arrangement which is used to remove the excess amount of ink from the rolls. Ink in the gravure roll transferred to transfer roll which is in contact with the substrate. Finally, by making low pressure contact, the transfer roll deposits the ink on the substrate. Figure 22 describes the arrangement of offset-gravure type printer. In this technology, ink solvent nature, viscosity, applied pressure and the material of the transfer roll play vital role in the finish quality of the print. However, the degradation of the doctor blade affects the printing quality and therefore proper selection of material for doctorable is important. This method commonly employed by application such as creating of radio-frequency identification (RFID) tags, TFTs, solar cells and sensors etc.

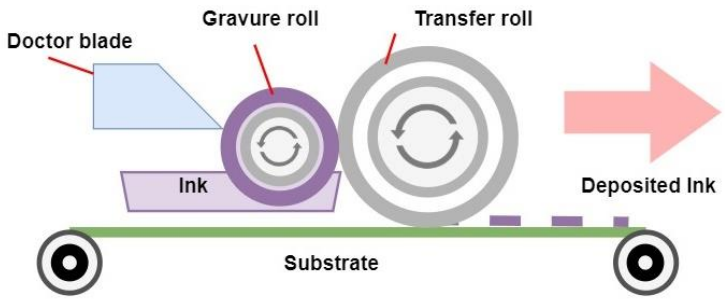

Figure 22. Offset gravure method.

3.5.6 Flexography

In this technology, the ink in the fountain roller is transferred to the anilox roll. The anilox roll which rolls in physical contact with the flexo roll is made with micro scale cavities in order to hold the e-ink. The contact between rolls transfers the ink to the flexo roll and it deposits the ink on the target substrate. Like in previous method, doctor blades prevent the over collecting exceed ink on the anilox roll [47]. The design circuit pattern is embedded on the flexo roll with the use of flexo plate. The low-pressure contacts on the substrate makes this method more suitable for wide spectrum of flexible substrates. This method is widely used for applications like e-labels, printed batteries etc [45]. Figure 23 describes the flexography printer arrangement.

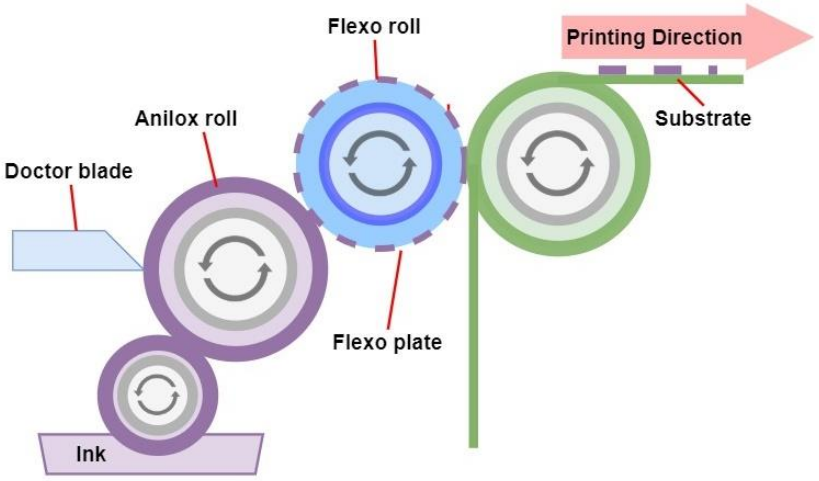

Figure 23. Flexography method.

3.6 Performance comparison of printing technologies

The performance of the above discussed technologies can be tabulated as below [45], [47].

Table 6: Performance of printing technologies

Printing method	**Line width /(µm)**	**Line thickness/(µm)**	**Speed /(m/Min)**	**Resolution /(µm)**
Inkjet	30 - 50	0.01 – 0.5	slow	15–100
Gravure offset	10 - 50	0.02–12	fast (1000)	50–200
Screen	30 - 50	0.02–100	medium (70)	30–100
Flexography	45-100	0.17 – 8	fast (500)	30–80

According to the Table 6, gravure offset, and flexography provide more fast production rate compared to others

3.7 Electrochromic displays

Electrochromic displays can be considered as another application of printed electronics. The structure of an electrochromic display is illustrated in Figure 24.

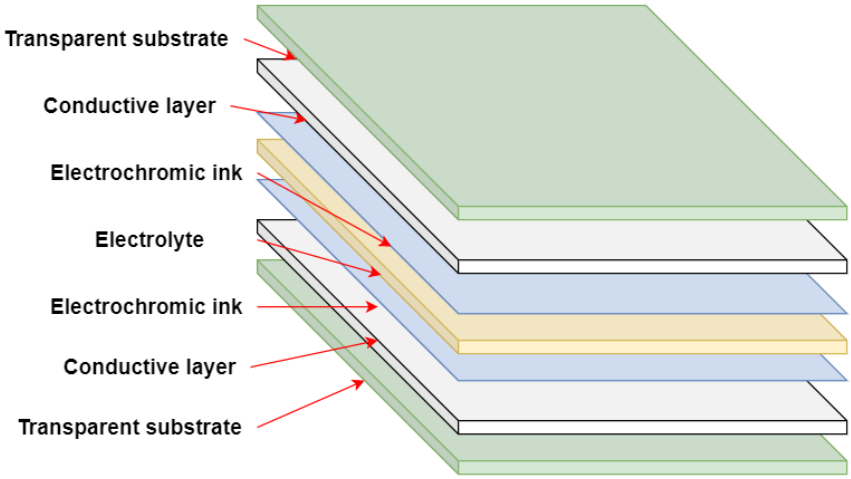

Figure 24. Structure of electrochromic display.

This display technology can be considered as semi bi-stable display technology which can hold the previous information for some time without consuming energy. When conductive layer is subjected to a voltage difference, the e-ink will move to the electrolyte and make visible the ink colour to the outside. When the conductive layer is subjected to a opposite polarized voltage, the ink will be redeposited on the substrate without showing any of its colour. In [48] authors have described multicolour electrochromic display technology which will upscale the demand for this technology. However, this display technology is constrained due to its limited ability of showing dynamic graphics and texts which are already achieved by other display technologies.

4 INTRODUCTION TO INDOOR ENERGY HARVESTING UNIT

Attaining the energy required for the operation of the wireless electronic nodes is one of the key challenges of this work. Small compact battery designs are vastly used as a feasible, effective solution for this task. However, battery solution comes with its own unique problems. Scheduled battery maintaining operations need to be carry out in order to get the service continually form the node. This will result in a considerable service cost and it is problematic when it comes to sensor networks with a large number of nodes. As a solution for that, more researches were conducted focusing on energy harvesting methods, allowing energy-autonomy. According to the authors in [9], sources like ambient light, vibration motion, thermal energy and RF can be used for energy harvesting. In addition, they have shown that the ambient light has an efficiency range of 5-30%, which is far beyond the other natural energy source efficiencies. Photovoltaic (PV) cells are used to harvest energy from the both indoor and outdoor ambient light.

4.1 Structure of energy harvesting system

The main structure of an energy harvesting system is described in Figure 25. The harvesters basically produce the energy conversion from renewable energy to electrical energy. PV cells, piezoelectric units, thermo electric units are examples of harvesters. Then conversion unit changes the voltage or current parameters of primarily produced power by using power electronics. Typically, buck converters and boost converters can be mostly seen on this type of conversion circuits. The power is then stored in the storage unit. Batteries and super capacitors are most commonly used for energy storing purpose. To coordinate between storage unit and conversion unit, a power management control unit is embedded to the system. In most cases, a specially designed integrated circuit (IC) will be used for this unit. In addition, generally the PV cell optimized power management units are manufactured with a maximum power point tracking (MPPT) feature, which always bias the PV input to obtain maximum performance.

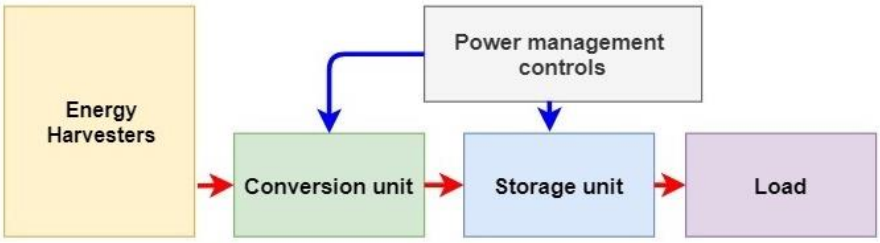

Figure 25. Structure of an energy harvesting system.

4.2 Photovoltaic cells

The main purpose of PV cells is the yielding of energy from the photons. Generally, the process of generating photocurrent falls in to two main processes.

a. Absorption of photons
b. Collection of charge carriers

The evolution of solar cell technologies can be breakdown to three generations

- First Generation Solar Cells: First generation photovoltaics use the highest purity materials such as crystalline silicon. This generation has the highest power-conversion efficiencies compared to others while as drawback, these are expensive to produce because of high processing costs to get pure materials.

- Second Generation Solar Cells: These PVs are based on low-cost, less complex preparation techniques such as vapor deposition and electroplating. As a trade-off, power conversion efficiency is lower compared to the 1st Gen. Nearly all thin film photovoltaics fall in this category. These PVs are made by using solar cells made up of multi-crystalline or amorphous Si, CdTe and Cd-In-Ga-Se (CIGS).

- Third Generation Solar Cells: This latest generation of these PVs is well-known for its physical characteristics of light weight, flexibility and low-cost manufacturing methods such as R2R. These includes PV technologies such as dye sensitized solar cells (DSSC), organic PV cells, etc.

Traditional 1st Gen and 2nd Gen solar panels work based on PN junctions in the PV cell. The photons emitted from sources, which have energy more than bandgap difference, get absorbed by the PV panel and generates electron-holes pairs. These get separated due to the electric field across the PN junction and this results in a photo current flow from the PV cell.

The operation of 3rd Gen photo voltaic cells takes a different approach. Their energy conversion relays on the formation of a heterojunction between the donor materials and acceptor materials. For this, manufacturers use organic semiconductor (OSC) materials such as organic dyes, polymers, small molecules and ensembles of semiconductor or oxide nanoparticles. Selection of material is subjected to the application of the organic PV cell. [49]. The structure of an organic PV cell is illustrated in Figure 26.

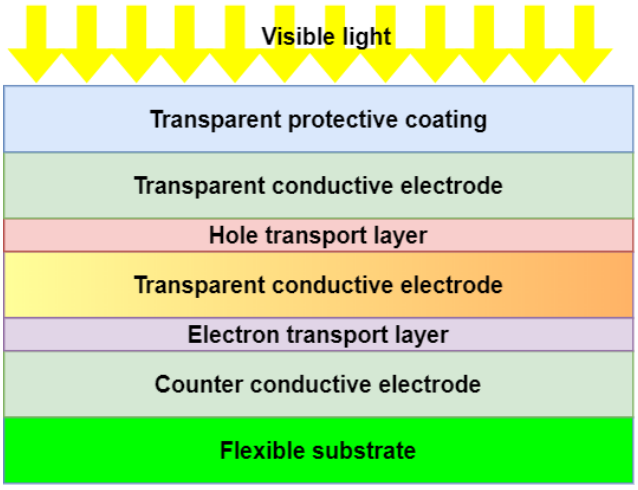

Figure 26. Structure of a flexible organic PV cell.

The operation of organic photo voltaic cell can be described as follows. According to Figure 27, visible light passes via the top transparent proactive coating of the solar cell and excites electron-hole pairs residing in the photoactive layer. This layer consists of both electron donors and accepters which are categorized based on their raw material properties. Due to the energy

which passed from light source, an electron-hole pair get separated and electrons migrate to the electron transport layer. This process results in an electric current in the conductor [50]

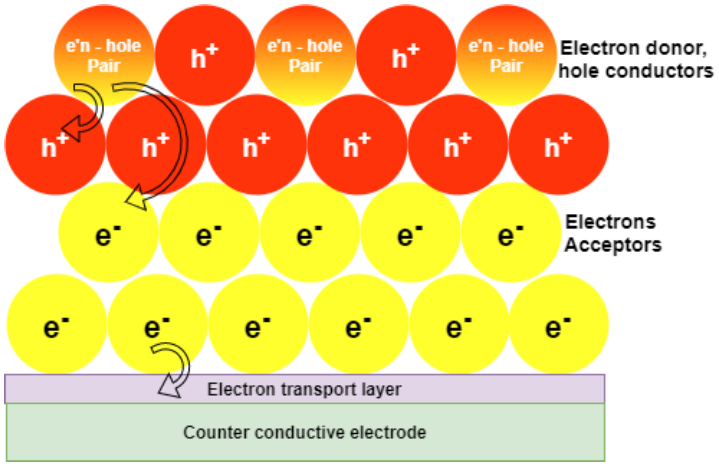

Figure 27. Summary of power generation in an OPV cell.

4.2.1 The equivalent circuit of a PV cell

Figure 28 describes the theoretical circuit model corresponding to PV cell which can be used to describe the electrical characteristics of the unit.

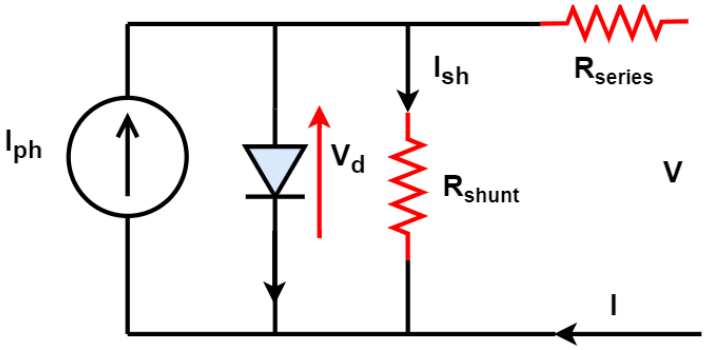

Figure 28. Equivalent circuit of a PV cell.

From the equivalent circuit, the load current can be obtained as,

$$I = I_{ph} - I_{sh} - I_d, \tag{19}$$

where,

I_{ph} = current produced by the solar cell; I_d = diode current; I_{sh} = shunt or leakage current; I = load current and V = voltage across load.

4.2.2 Performance parameters of PV

Performance of the PV cells can be compared based on their own power conversion efficiency value. High PV power conversion efficiency leads to minimum amount of PV cell area which required to power-up the application device. By considering the concept of ideal PV cell which consists of a constant current source, a diode and a load, the parameters can be expressed as follows. In here, PV cell is assumed to be operated as a current generator when the surface is exposed to a light source [51]. The power conversion efficiency (PCE) of an orgonic solar cell can be given by

$$PCE = \frac{I_{SC}\, V_{OC}\, FF}{P_{in}}, \tag{20}$$

where $$\text{FF} = \frac{I_{MPP}\, V_{MPP}}{I_{SC}\, V_{OC}}\text{, (MPP – Maximum Power Point);} \tag{21}$$

I_{SC} represents the short circuit current,
V_{OC} - open-circuit voltage, FF - fill factor, and P_{in} is the incident solar power.

further, open circuit voltage can be expressed as

$$V_{OC} = \frac{n\, k_B\, T}{q} \ln\left(\frac{J_{ph}}{J_0} + 1\right), \tag{22}$$

where k_B - Boltzmann constant; J_{ph} - Photo current density; J_0- Reverse saturation current density and T – Temperature;
The above-mentioned parameters are illustrated on the I-V curve of a PV cell, as shown in Figure 29.

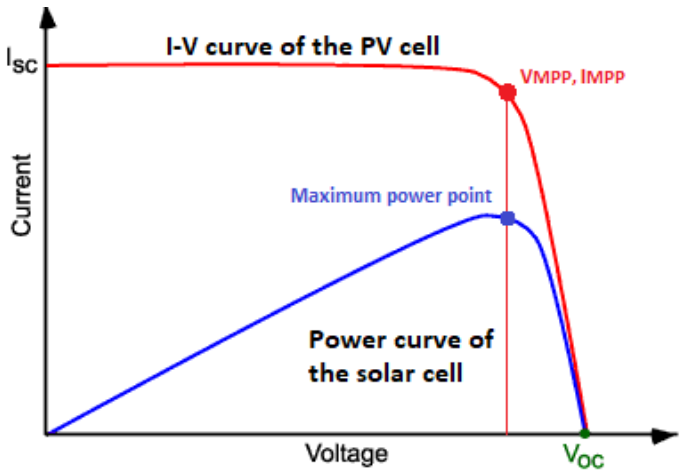

Figure 29. I-V curve of PV cell.

According to the graph, when a load is attached to the PV cell, the terminal voltage is expected to be dropped below V_{OC} value. The PV cells have the ability to provide constant current till the cell reach to maximum power point. At maximum power point, the PV cell provides its maximum power generation to the load. Generally, the maximum power point

exists on 80% of V_{OC} value. According to the [52] [53], performance of different solar generations can be tabulated as below

Table 7 : Solar conversion efficiency for various photovoltaic systems

Generation	PV material	Typical efficiency
1st	Si (crystalline)	26.7 ± 0.5 %
	GaAs (crystalline)	26.1 ± 0.8 %
	InP (crystalline)	24.2 ± 0.5 %
2nd	Si (thin film)	16.7 ± 0.4 %
	GaAs (thin film)	26.1 ± 0.8 %
	CIGS (cell)	19.4 ± 0.6 %
	CdTe (cell)	16.07 ± 0.5 %
3rd	Dye sensitized	10.4 ± 0.3 %
	Organic	9.7 ± 0.3 %
	Perovskite	23 %

According to the Table 7, the Perovskite PV cells have the best efficiency compared to the rest of 3rd generation PV cells. This fact highlight that PE-based PV technologies can deliver high efficiency energy conversion performance while preserving their unique flexible and cost-efficient characteristics.

4.2.3 PV cell performance under indoor lightning

The study in [54], shows a comparison of efficiency in commercially available organic, dye sensitized, a-Si PV technologies under indoor tri-phosphor fluorescent source illumination condition. Their results can be tabulated as shown in Table 8.

Table 8: Efficiency comparison under indoor illumination

Lighting condition	Normalized efficiency of PV device		
	OPV	DSSC	a - Si
TL84 NB: (tri-phosphor fluorescent source (4100K))	0.45	1.35	0.50

Based on above results, it can be concluded that dye sensitized PV will outperforms other commercially available PV technologies under indoor lighting conditions.

4.2.4 PV cell arrangement

The PV cells can be arranged by two ways as described in Figure 30. In series configuration, negative and positive terminals of adjacent PV cells have connected each other, and one positive and negative connection attached to the load, while in parallel configuration all positive and negative terminals are connected to the terminals on the load.

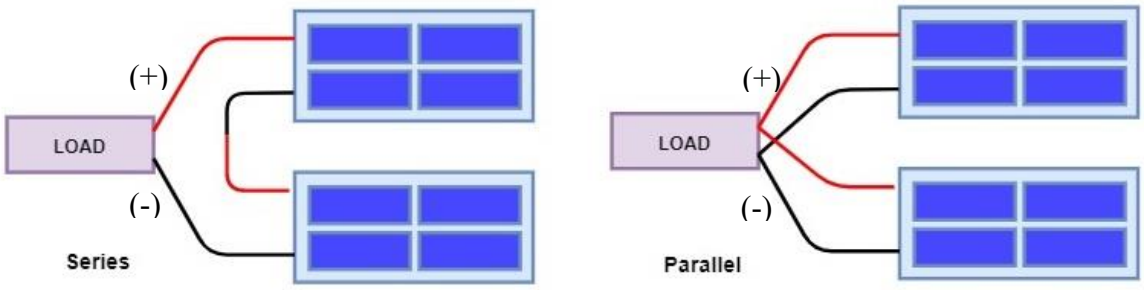

Figure 30. Series and parallel PV cell arrangements.

These two methods have their unique characteristics are displayed in Table 9.

Table 9: Series and parallel configuration comparison

Series configuration	**Parallel configuration**
Suitable for large terminal voltage requirement. Voltages of each cell will be added while keeping constant current through all cells.	Suitable for large current voltage requirement. Current output of each PV cell will be added while keeping constant voltage between the common terminal.
As number of cell unit increases, drawing current will be limited to the total internal series resistance.	Terminal voltage will be limited based on the lowest terminal voltage PV cell in the array.
Different rated voltage cells can be used.	Similar rated voltage cells need to be used.
Drawing current will be limited based on lowest rated PV cell in the array.	

The above facts suggest the importance of using similar rated PV units in order to maximize the efficiency of the solar array.

4.2.5 The effect of angle with indoor light sources

The angle of incident has a direct impact on the generation efficiency of PVs. According to research carried out regarding this, it turns that the PV achieve its best performance when they are angled between approximately -30 to +30 from normal to the PV surface [55]. The effective angle of receiving for a PV is illustrated in Figure 31.

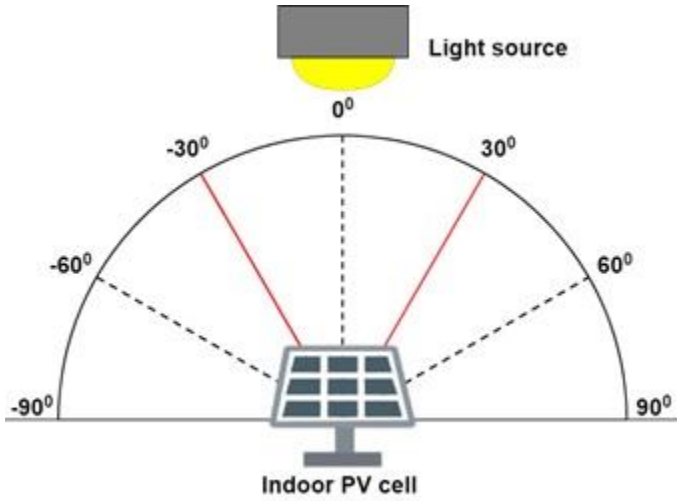

Figure 31. Angle reference with indoor light sources.

5 DESIGN AND IMPLEMENTATION OF A LIOT NODE

In this project, the protype is expected to be used as product information display (Figure 1). The implementation was based on the structure illustrated in Figure 32. A transmitter unit and two receiver nodes equipped with different display technologies were developed under the design requirements. In generally, the prototype was designed as a low power, energy-autonomous LIoT node. The display in the node is expected to update the contents based on the received data from the VLC link. In addition, multiuser communication is supported, that is, receiving LIoT nodes can be addressed independently by the transmitter and PV cell-based data reception.

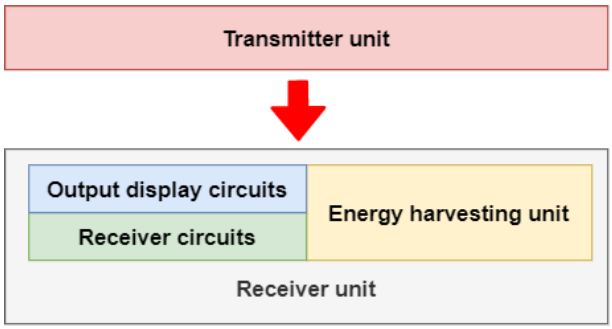

Figure 32. Prototype main structure.

5.1 Transmitter

In the designed prototype, the transmitter unit was designed by using several main units. They are; microcontroller unit (MCU), LED driver, power chip on board power LED (COB).

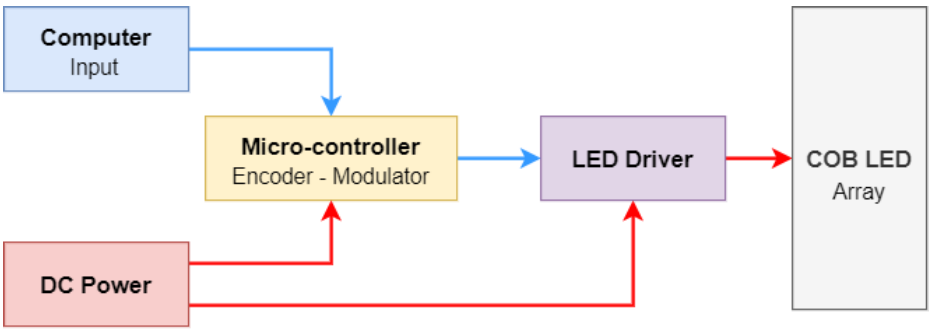

Figure 33. Prototype transmitter structure.

Referring to the Figure 33, the computer input data is fed into the microcontroller by using serial communication. The input data are dispatched with a combination of both multiuser identification and the payload (i.e., information to be displayed). A Matlab environment-based computer program was designed to take user identification (ID) and payload data from graphical user interface and then translate the input raw data into machine level. The processed data are transferred to the microcontroller through USB serial communication. Thereafter, the microcontroller encodes and modulates the received data according to the PPM based RECS-

80 protocol and then the modulated signal waveform is sent to the LED driver. The LED driver drives the transmitting COB LEDs according to the modulated signal. The whole transmitter system is powered by an external power supply. The concerned selection criteria for design of each unit are described below.

5.1.1 Modulation

In this design, for the data transmission, pulse position modulation (PPM) was used. Since PPM uses a high level to represent both bit 0 and bit 1, it naturally assists to reduce flickering effects in VLC systems. The data frames were based on the RECS-80 protocol which is also known as the old Panasonic infrared protocol. Its ability of carrying a large number of multi addresses was mainly considered when selecting the protocol. The binary bit representation of used PPM is shown in Figure 34.

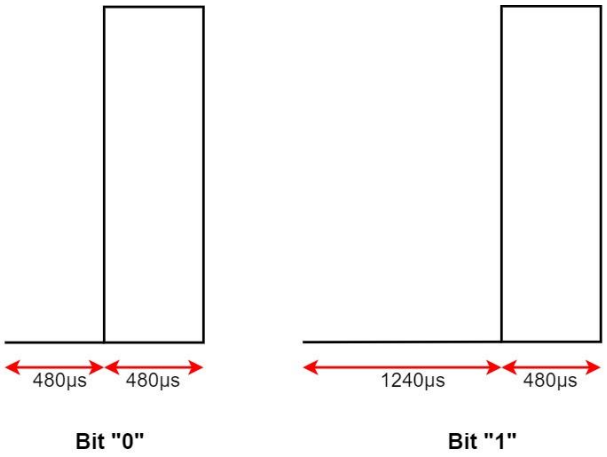

Figure 34. Bit representation according to PPM used in RECS 80.

These pulses were generated using a 38 kHz carrier signal in order to distinguish the data signal from environment noise. In this way the receiver can filter out the incoming signal using around 38 kHz region filter and extract the less noisy data signal. The modulated signal contains 48 bits (excluding start and stop bits) while it consists of address and data parts. The address part is used to facilitate the multiuser requirement. In this design, the address part contains 16 bits which can create 65536 distinguishable addresses. These can be utilized for multiuser scenarios or multi tagged data scenario for the same user. The data part contains 32 bits for the data payload. An oscilloscope-captured waveform of the transmitted signal is depicted in Figure 35.

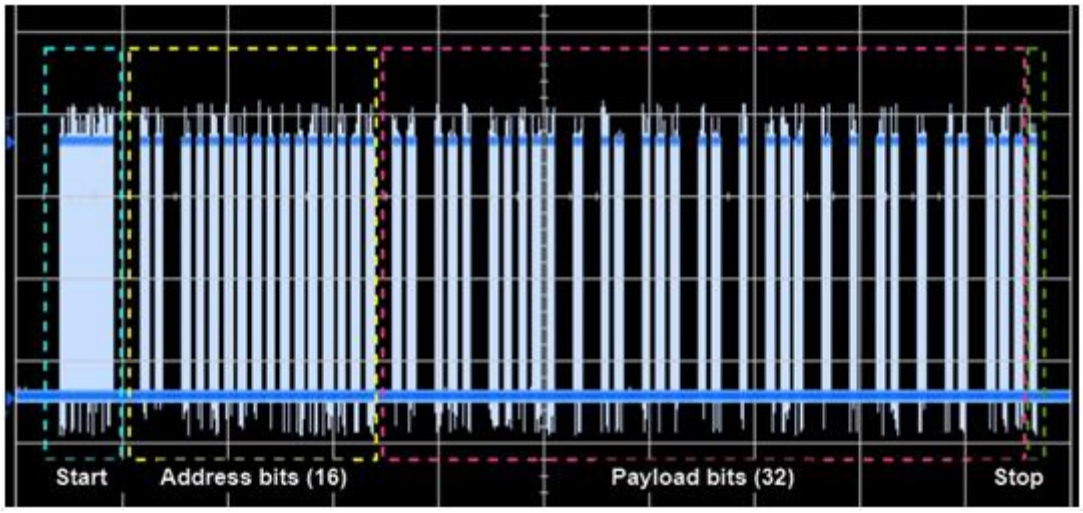

Figure 35. Data frame according to RECS 80 protocol.

In the prototype, address bits were used to facilitate 256 multiusers and 256 sperate tags for each user.

5.1.2 Transmitter's Microcontroller Unit

In this prototype, the MCU was used to perform as encoder and modulator in a typical VLC system architecture. Since the transmitter unit is expected to be stationary and connected to the powerline with infrastructure for all the time, no power constrains were considered. Hence no special power saving techniques were followed when design the data transmitting algorithms. The selection of MCU for the transmitter was made based on the following criteria.

- Its ability to generate the 38 kHz carrier signal precisely (clock speed)
- User friendly serial communication capability – integrate with computers and use Matlab environment for performance evaluation and troubleshoot easily.
- User friendly serial communication capability – integrate with computers and perform debugging tasks without additional circuitries.
- Number of general purposes, input, output (GPIO) pins
- Commercial availability

Based on above criteria, the ATmega328P MCU based Arduino Uno development board was selected to implement the transmitter prototype. C language-based Arduino integrated development environment (IDE) and Matlab environment were used for the programming purposes of the transmitter.

5.1.3 LED driver

For the design of LED driver of the transmitter, the following criteria were considered.

- Fast switching ability to generate detectable carrier signal.
- Handling high power for COB type power LEDs – COB require large current compared to the other circuitries. (>1000mA)
- Expected to respond Transistor–Transistor Logic (TTL) level output coming from MCU's output.
- Commercial availability.

In order to facilitate above requirements, as the current driving unit, a N channel metal–oxide–semiconductor field-effect transistor (MOSFET) was chosen. IRF520 N channel MOSFET was used in the LED driver circuit. The key specifications of IRF520 are listed in Table 10, which are aligned with prototype design requirements.

Table 10. Features of IRF520 N MOSFET

Feature	**Rating**	**Remarks**
Drain-source voltage	100 v (max)	Useful to provide sufficient large DC voltage for COB LEDs
Gate-source voltage	± 20 v(max)	Microcontroller output signal (TTL level 0-5v) can be directly fed to the transistor without any amplification.
Continuous Drain Current	6.5 – 9.2 (A)	Useful to provide sufficient large DC Current for COB LEDs
Rise and fall time	20 – 30 ns	This enables MOSFET to support high frequency DC pulses which is well with the design data rate requirement

The circuit diagram of the LED driver is described in Figure 36. To detect at the gate input of the MOSFET, the output of MCU's was programmed to generate modulated TTL level signal. In order to achieve better modulation bandwidth and modulation index, a bias voltage was added to the input voltage. An additional series diode was connected to the circuit to protect MCU's output pin from bias voltage. When the gate voltage level fluctuates according to the modulated signal, the MOSFET will draw current corresponding to the gate voltage variation.

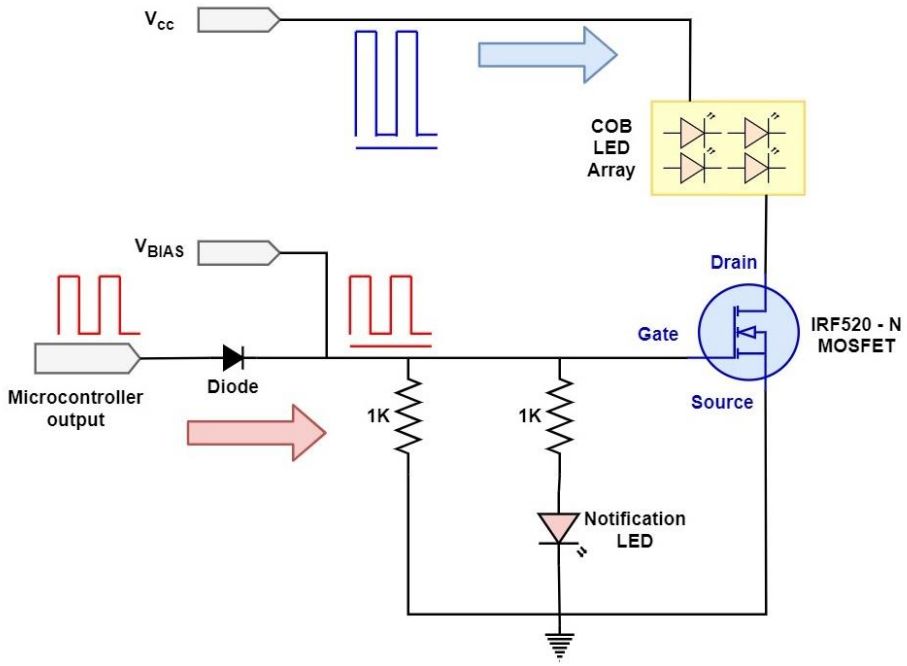

Figure 36. Design of the LED driver circuit arrangement.

5.1.4 Light source – LED

The prototype was based on the concept of energy-autonomous IoT with VLC. Therefore, from the transmitter end, the light source is expected to deliver detectable visible light signal with suitable colour wavelength for the indoor illumination and providing enough light energy to be harvested. Hence, the selection of LED was based on the following criteria

- Sufficiently fast rise and fall time characteristics.
- PV cell friendly wavelength emitting LED for efficient harvesting. (light temperature)
- Human eye pleasant colour for use the transmitter as a day-to-day illumination device.
- Feasible voltage and current requirement for less complex transmitter design
- Commercial availability

According to the study carried in [56], researchers have shown that the indoor light-based blue colour (wavelength 400−525nm) can produce energy more efficiently on PV cells. Based on that fact, the Kelvin colour temperature of the transmitting LEDs were determined by using the Wien's displacement law. Even though LED does not directly follow the Wien's law due to electroluminescence process of illuminating, it still provides a clue regarding emitting wavelengths from the LED [57]. The manufacturer provided colour temperature and their wavelength regions are illustrated in Figure 37.

The expression for the Wien's Law can be written as

$$\lambda_{max} = \frac{2.898*10^{-3}}{T}. \tag{23}$$

By assigning the wavelength as 480nm, the equation provides Kelvin temperature rating of 6000K as the results.

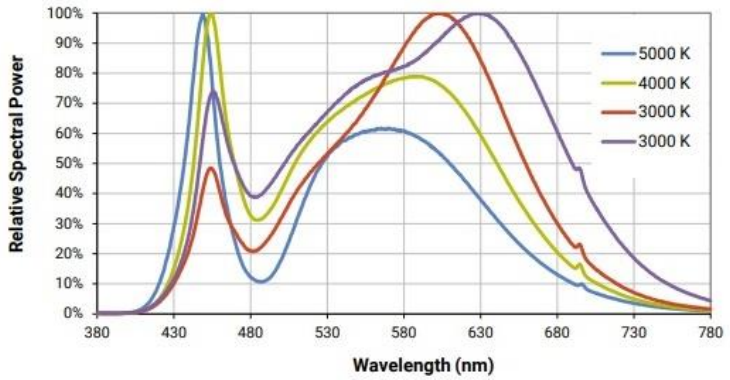

Figure 37. LED temperature and their wavelengths [58].

In addition, since COB LEDs are made of with small compactly arranged multiple light emitting diodes, they can facilitate a greater number of lighting sources in given area compared to the traditional surface or through hole mount LEDs. Therefore, based on above facts, 5700K COB type LEDs were chosen as the lighting source for the transmitter.

5.1.5 Transmitter algorithm

The transmitter algorithm can be described as in the flow chart shown in Figure 38. The implemented programming codes are crated based on this algorithm using both Arduino and Matlab environments.

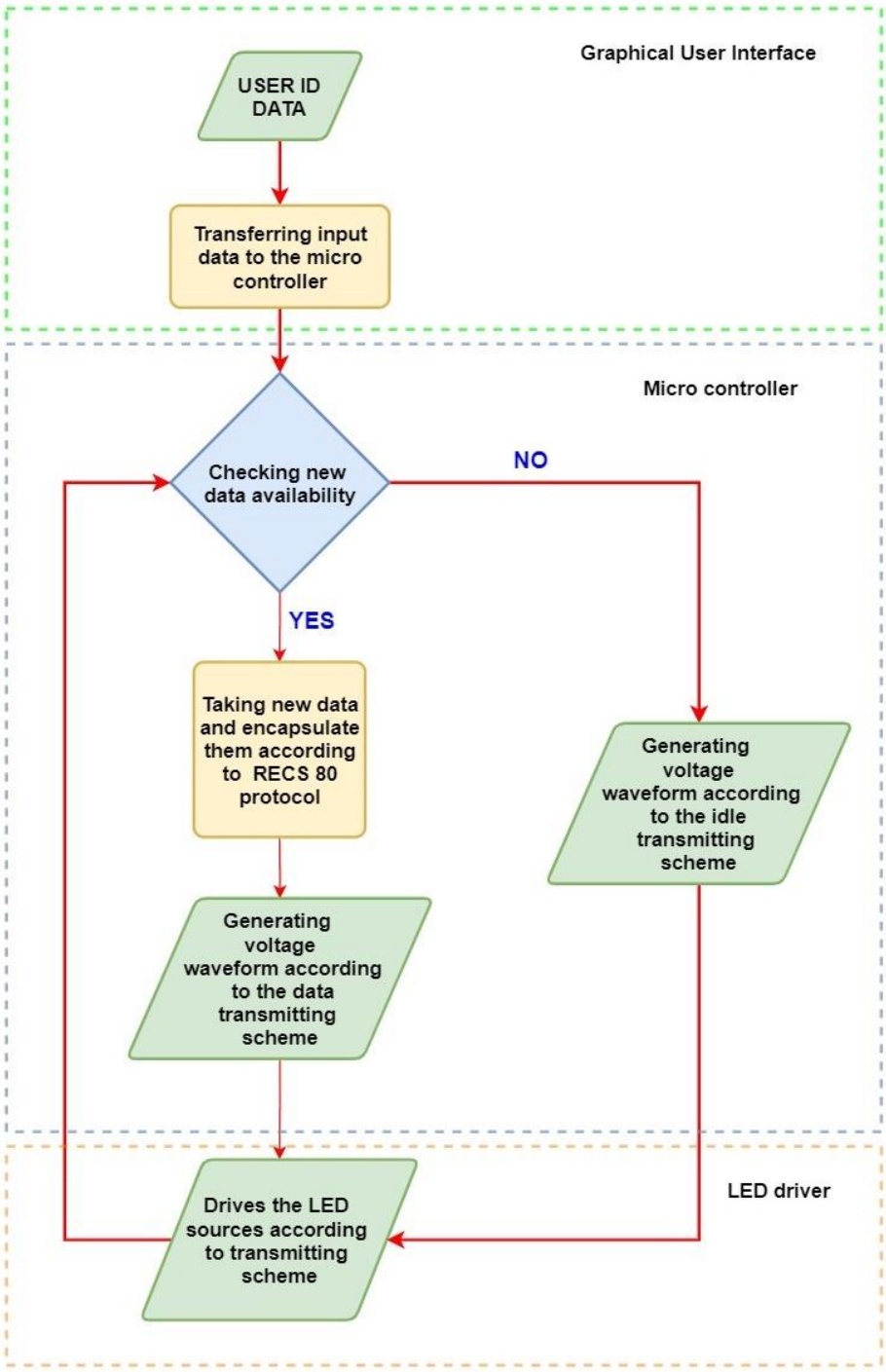

Figure 38. Transmitter algorithm flow chart.

The designed graphical user interface (GUI) for the prototype is shown in Figure 39. The GUI is designed in order to facilitate the multiuser scenarios with multiple data under different data tag. Final input for the transmitter MCU is created based on the user number, input data and the data tag under the command button.

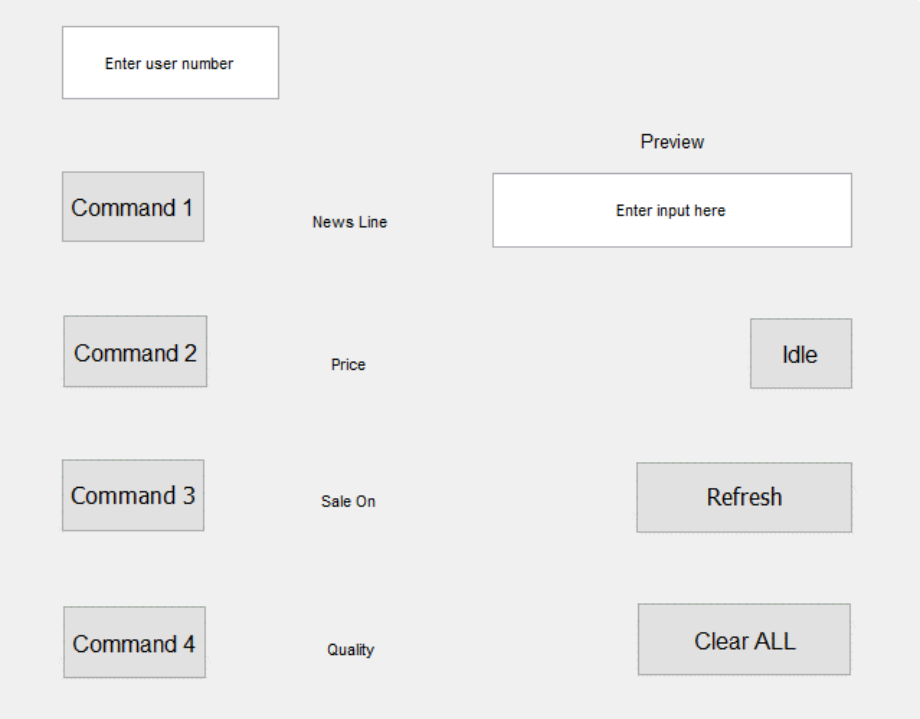

Figure 39. Graphical user interface for the transmitter

The transmission scheme was designed to provide maximum illumination when there is no data transmission for the receiver (idle state). An oscilloscope-captured waveform of two transmitting schemes is shown in Figure 40.

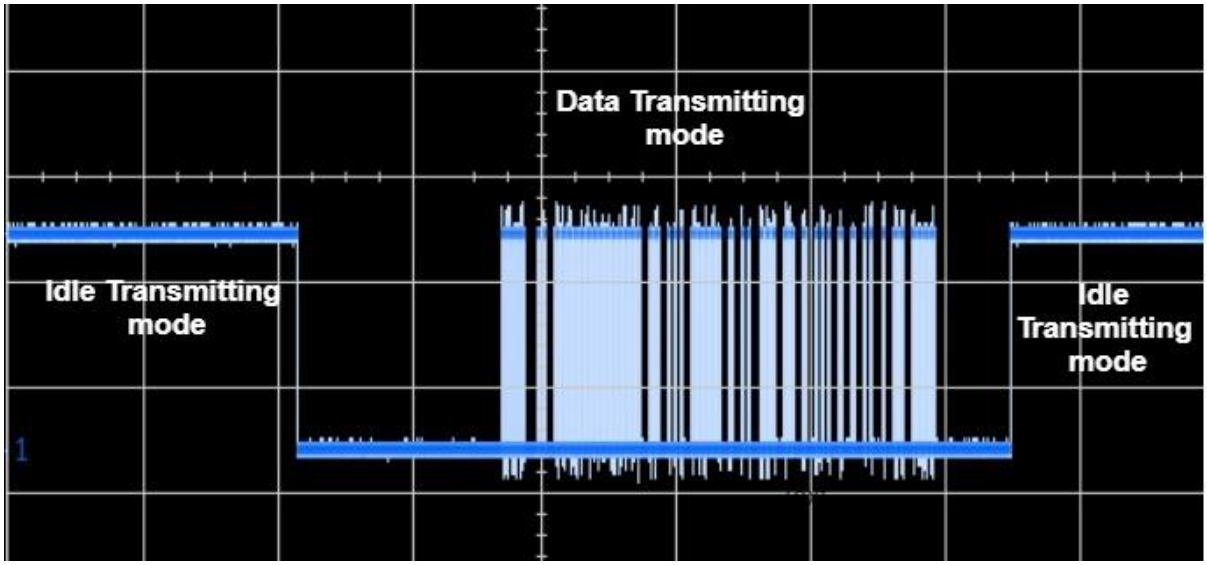

Figure 40. Transmitting schemes.

5.2 Receiver

The receiver of the system is made up with several components. Receiving circuit, MCU and display unit were the main units of the prototype design. In addition, the energy harvesting unit is also placed with the receiver circuitries.

5.2.1 Receiving circuit

The receiver circuit was designed to receive the visible light-based waveform and filter out the 38 kHz modulated data signal. The final output of the signal was expected to between the range of TTL levels so that MCU's analogue to digital converter (ADC) can directly sample them without any further rectifications.

In this project, two possible receiving technologies were tested. In addition to traditional photodiode approach, PV cells in the energy harvesting unit were tested to receive the VLC signal while energy harvesting.

5.2.2 Photodiode based approach

The receiving circuit is shown in Figure 41. The photodiode receives the visible light-based signal and generates current signal corresponding to the light waveform. The transimpedance amplifier converts the current signal into a voltage signal so that, any signal processing function can be applied on that. The automatic gain control amplifier (AGC) amplifies the signal to keep constant stable voltage levels in the voltage signal. Then, the voltage stabilized signal waveform forward to the 38 kHz region bandpass filter in order to eliminate all noise effects and extract the transmitted 38 kHz modulated signal. The output signal is fed into a switch mode-configured transistor, in order to provide TTL voltage level (3.3V) to the MCU's ADC for sampling purposes.

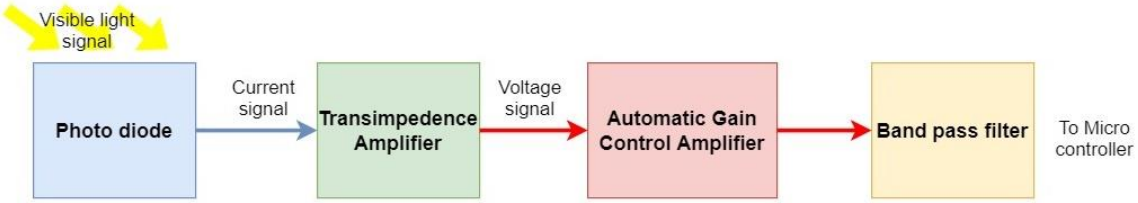

Figure 41. Receiving circuit structure.

A PIN type photo diode was used as the photodiode for the prototype. A VSOP38338 IC was selected as the amplifying and filtering unit, as the IC comes with all required blocks for the purposes.

5.2.3 PV cell-based approach

The PV cell-based receiver circuit was made to filter and extract data signal from the received DC biased wave form. Since, the output of this circuit is expected to be fed to the same programmed MCU, the outputs of both circuits (photo diode and PV cells) were expected to be identical. The structure for the PV cell-based approach is described in Figure 42.

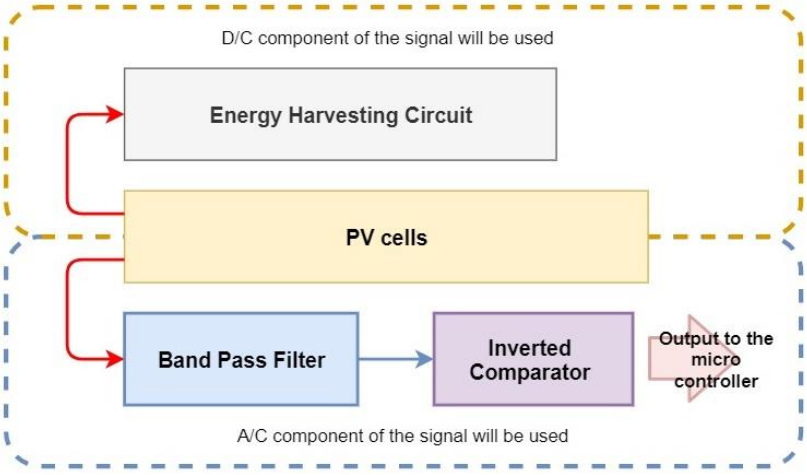

Figure 42. PV cell-based receiver structure.

For the receiving circuit, A/C voltage component will be used. The A/C waveform will be filtered with the bandpass filter in order minimize the noise and extract the transmitted signal form the A/C waveform and then it will be fed to an inverted comparator in order to stable the voltage levels to TTL level. The inversion of the signal will be used to comply with the RECS80 protocol. The design of the 1st order active non inverted bandpass filter was based on the follow equations

$$f_{L.cutoff} = \frac{1}{2\pi R_2 C_2}, \tag{24}$$

$$f_{H.cutoff} = \frac{1}{2\pi R_1 C_1}. \tag{25}$$

The design architecture for the active non-inverted band pass filter is illustrated in Figure 43.

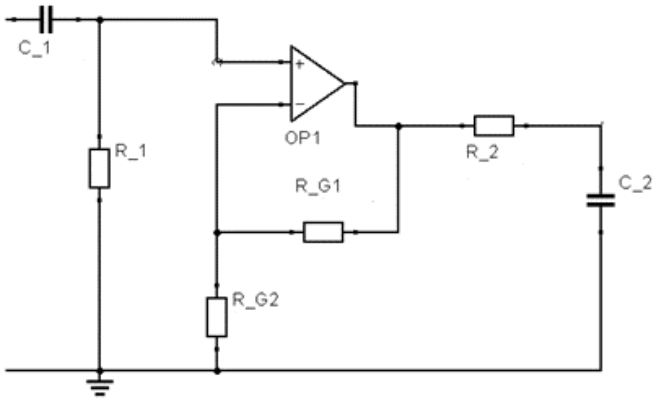

Figure 43. Non inverted bandpass filter for signal extraction.

5.2.4 Receiver's Microcontroller Unit

In the receiver design, the MCU was expected to serve as the decoder and the demodulator of the receiver. Moreover, since the IoT node is expected be energy-autonomous, efficiency and low power input characteristics were prioritized when selecting the MCU. The considered selection criteria for the MCU is shown below

- Low power consumption
- Sufficient ADC performance for sampling
- User friendly serial communication capability – integrate with computers and perform debugging tasks without additional circuitries.
- Number of GPIO pins in order to attach with output devices (displays)
- Commercial availability

Based on above criteria, the ATmega328P MCU-based 8MHz 3.3V power optimized Arduino pro mini development board was used.

5.2.5 Display device

In the prototype receiver design, displays were used as the output device of the node. The following criteria were considered when selecting the display

- Low power design
- Compatibility with the MCU
- Flexibility and compact design for any surface integration
- Less complex biasing/ excitation circuitries for operation
- Commercial availability

As the candidates for this task, electronic ink (e-ink) and printed electrochromic display technologies were considered. Their bi-stable characteristics fulfilled the low power design requirement. Bi- stable displays have the ability to keep last updated information in their display interface for longer time without any power consumption. This enables the micro controller to keep power consumption to a minimum at idle state. When new data arrives, the display is automatically refreshed, and it will print the information on display area. In the design, "ADAfruit e-ink 2'7" display with display driver and" Ynvisible" electrochromic display was used. In the display driver-based e-ink display, the driver uses serial peripheral interface (SPI) to communicate between the MCU and the output. The library and receiver programming codes were developed to decode the received data to American standard code for information interchange (ASCII) format and then print it on the e-ink display. The final appearance of the e-ink display unit is shown in Figure 44. Since the electrochromic seven segment display did not require any driver for its operation, it was directly connected to the MCU. In order to preserve the bi-stable nature of the display for longer period, a pull up resistor arrangement was used at the MCU output pins. The electrochromic printed seven segment display is shown in Figure 45.

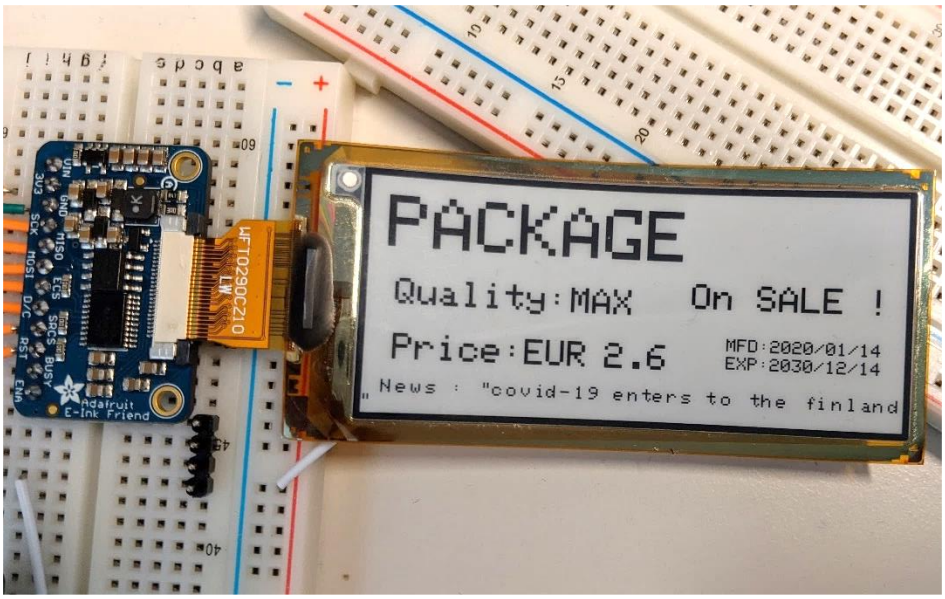

Figure 44. E-ink display and driver unit manufactured by Adafruit Industries.

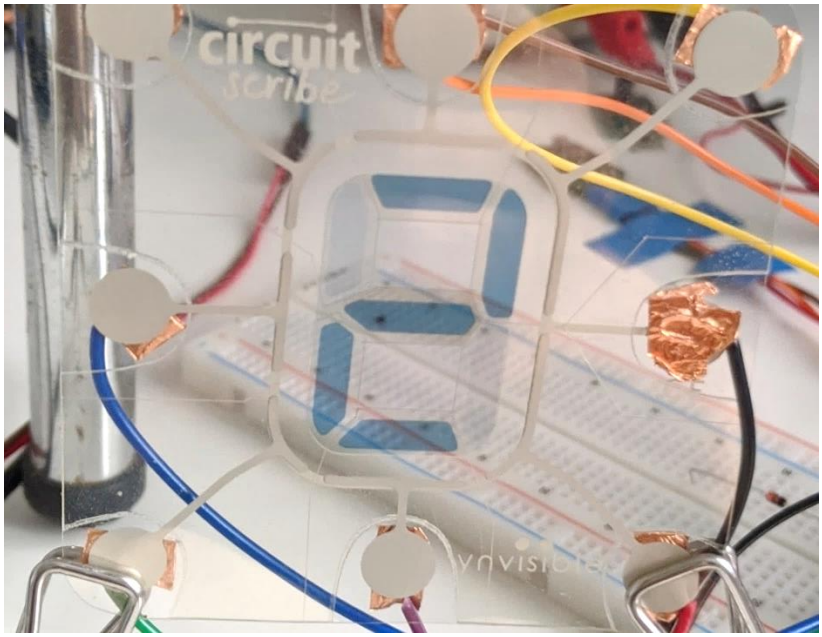

Figure 45. Electrochromic seven segment display developed by Ynvisible.

5.2.6 Receiver algorithm

The designed algorithm for the receiver is illustrated in Figure 46. Initially, the receiver is expected to scan continuously till valid data signal is available. As soon as a valid signal is present, it will be separated to the main components of user ID, tag ID (data label), and data payload. The algorithm will check for correct user ID match for obtain user confirmation and then the user confirmed data will be forwarded to target data tag. Finally, after the confirmation

of tag, the received payload data will be converted to ASCII characters for obtain meaningful information to the users and it will be printed on the display.

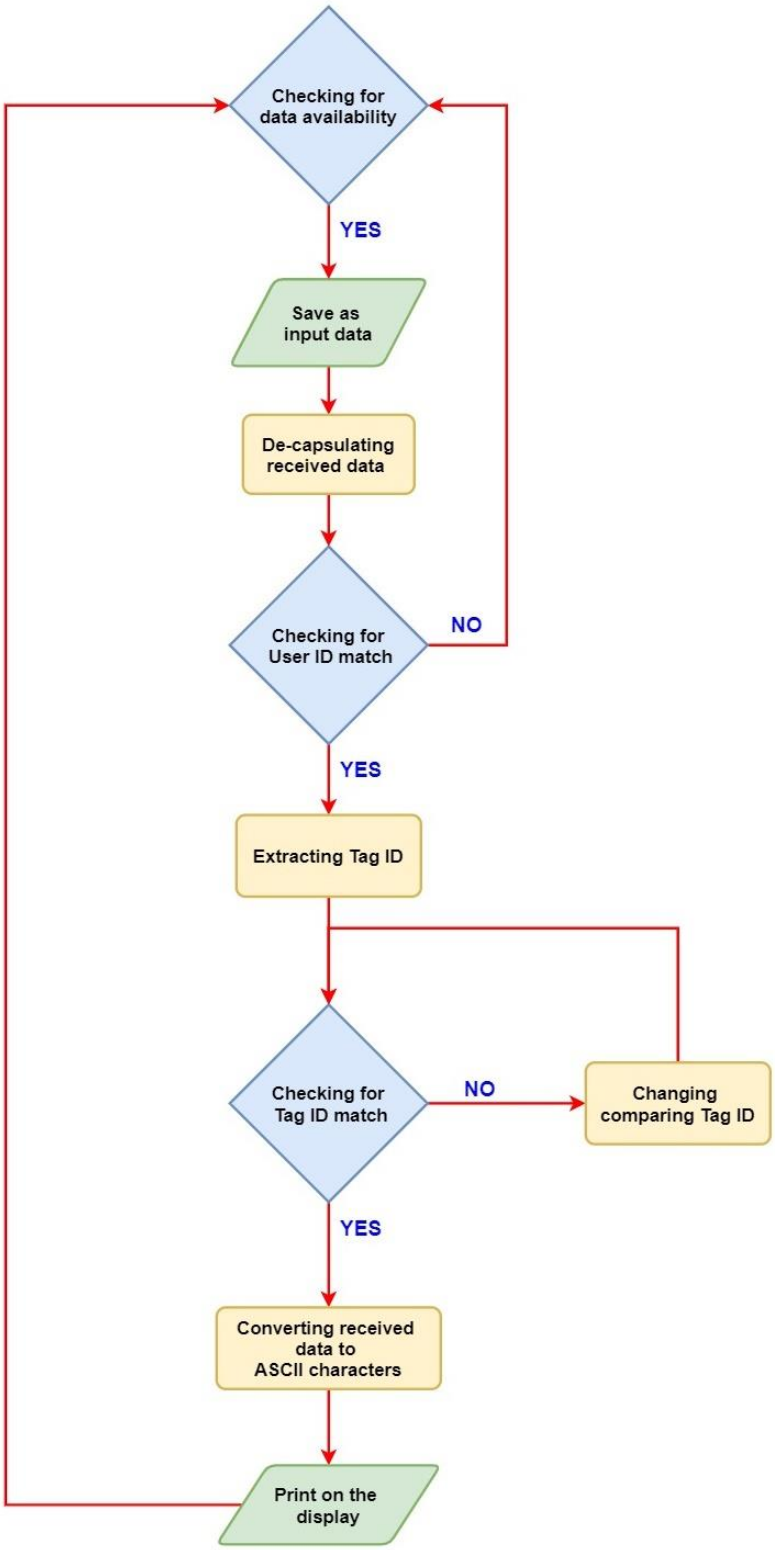

Figure 46. Receiver algorithm.

5.3 Energy Harvesting unit

The harvesting unit was designed to harvest energy from the indoor illumination created by the transmitter. For the prototype, multiple printed flexible PV cells were tested to make the design easier to integrate on any kind surface. In order to preserve the concept of "expose and connect", initially the harvesting unit was designed without using any kind of large energy storing devices i.e., supercapacitors, batteries. Using energy storage devices will challenge the expected compact flexible design while limiting the expected applications due to their constrained working temperatures and conditions.

To provide sufficient power for the MCU, feasibility of both series and parallel PV configurations were tested. In series PV cell arrangement, large currents draw by the MCU, resulted significant voltage drop due to the cumulated series resistances. To mitigate that, the prototype's microcontroller was powered up by a parallel configuration. As a disadvantage of this arrangement, a large area of printed PV cells was required for satisfy the power requirement. The simple design for this approach can be seen in Figure 47. In this design, a diode protection arrangement was used to protect PV cells. A small-scale electrolyte capacitor was used to regulate the effects caused by voltage fluctuations during data transmitting schemes. The selection of capacitor value was estimated according to the below equation

$$R_{Load} * C >> \frac{1}{f}, \tag{26}$$

where; R_{Load} = load resistance, f = DC ripple frequency and C = capacitance

The organic PV cells manufactured by Infinity PV were used for the design.

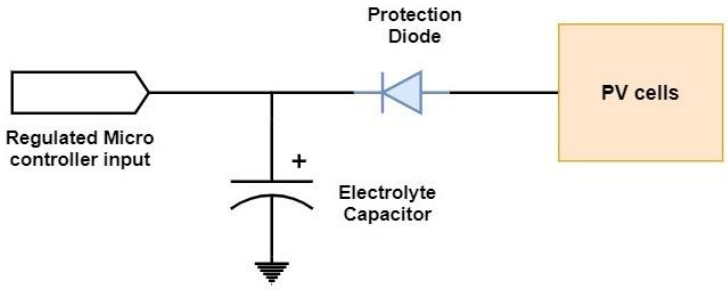

Figure 47. Direct energy harvesting circuit.

However, to provide sufficient power using minimum size of PV cells, the feasibility of using an energy harvesting unit were tested. Since, the transmitters were designed to provide more constant illumination throughout operation, features like MPPT harvesting methods were not prioritized. The energy harvester was selected based on the below criteria

- Sufficient power output for receiver microcontroller and other components power requirement.
- Low current consumption from PV cells in order to avoid voltage drop due to series resistance.
- Less power storage design for preserve the concept of "expose and connect" much as possible.

Based on above criteria, the LTC 3588 energy harvesting chip was selected. The final energy harvester-based design is shown in Figure 48.

Figure 48. Energy harvesting circuit with energy harvester IC.

According to this design, the output from PV cells will be stored in the super capacitor arrangement. In this way, due to low current intake from energy harvesting IC, sufficient energy for MCU's operation will be stored in the supercapacitors. Then harvester IC is expected to save the configured amount of energy in the internal capacitor. internal capacitor will directly provide the energy requirement for the connected load. Whenever the internal capacitor voltage goes below the configured value due to the consumption, the harvester IC will recharge it by transferring energy from supercapacitors based on its optimized algorithms. In case of PV cells cannot provide sufficient rate of energy for the load's requirement, the harvester circuit will cut off the power supply to the load enabling time window to recharge primary storage supercapacitors up to a configured voltage. After reaching the "turn on" threshold voltage, the harvesting circuit will turn on the power supply to the micro controller till it goes down to the "cut off" threshold voltage. The configured values for the prototype are given in below Table 11.

Table 11: LTC3588 configured voltages

Threshold	**Voltage threshold at super capacitor /(V)**
Cut-off	3.3
Turn on	5.14

The capacitors for the harvesting unit were selected as follows. According to the [59] , charge on a capacitor is can be obtained by from the expression

$$Q = C * V, \tag{27}$$

where; C= capacity, V= voltage

The time constant for RC is defined as

$$\tau = R * C, \tag{28}$$

where; C= capacity, R= series resistance.

Since a capacitor typically takes five times of time constant to be practically fully charged, according to the equation (28) it is important to keep both R and C values minimum in order to keep the time constant minimum. However according to the equation (27), to store sufficient energy for receiver's operation, it is important to keep sufficient capacity and terminal voltage

in the setup. Since the terminal voltage of the capacitor is fixed due to the PV cell output voltage value the capacity should be selected to satisfy the energy requirement. Therefore, the selection of supercapacitor values was made based on taking the optimum value between the trade-off of charging time and the charge capacity. Large capacity supercapacitors can keep enough power to run the circuits for longer period while taking considerably large time for initial charge up. To minimize the power loss during the storing, super capacitors with low leaky currents were selected for the final design.

6 PERFORMANCE EVALUATION

The performance of the implemented prototype designs are evaluated and discussed in this chapter.

6.1 Transmitter and photodiode receiver waveform

The transmitted (top) as well as received and filtered (bottom) waveforms following the RECS80 protocol are shown in Figure 49.

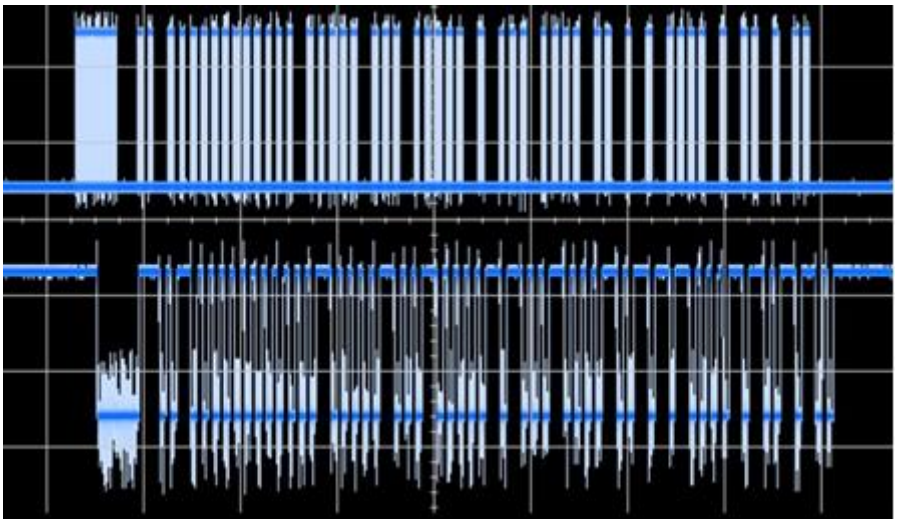

Figure 49. Transmitted and received waveforms.

As observed, the received waveform is the inverted version of the transmitted waveform. Since, at the quiescent state, the photodiode circuit is keeping the voltage on high level and as a result of that, the output waveform gets inverted.

6.2 BER performance of the receiver.

The bit error rate (BER) performance was measured under for two different scenarios. One measurement was taken near by a window place, where non direct sunlight is present in order to superimpose the ambient noise with the VLC signal. To calculate BER, the following basic version of equation was used.

$$BER = \left(\frac{Number\ of\ errors}{Total\ number\ of\ bits}\right). \quad (29)$$

Typical 50Hz flickering in an indoor illuminated place was chosen as the second environment. The transmitter was placed above the photodiode receiver when taking the measurements. In both measurements LoS links were utilized. The vertical distance between transmitter and photodiode was changed during the experiment. The results are plotted in Figure 50. The used algorithm for BER calculation is attached in appendix 1.

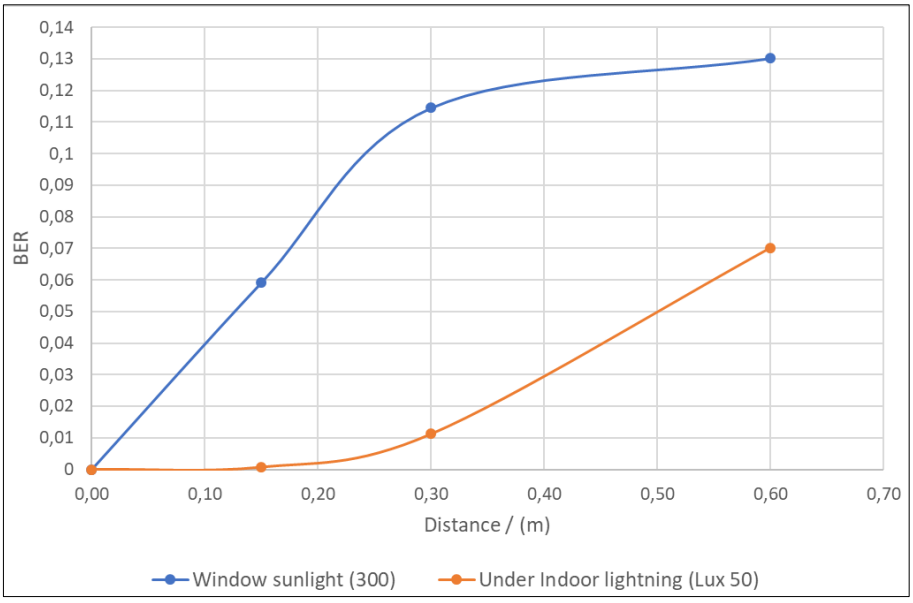

Figure 50. BER vs distance under different noise environment.

The results suggested that, the photodiode-based receiver performs well under the indoor illuminated scenarios compared to natural lighting scenarios. From the graph we can observe that, when the transmitting distance is below 20 cm from the receiver, the photodiode-based receiver's BER is acceptable for proposed indoor application under any light scenarios.

6.3 The performance evaluation of printed PV cells

For the experiment, two different R2R printed PV cell technologies were tested. Gravure printed perovskite cells and printed organic cells were used for obtaining the following results. The used samples of PV cells are attached in Figure 51 and Figure 52.

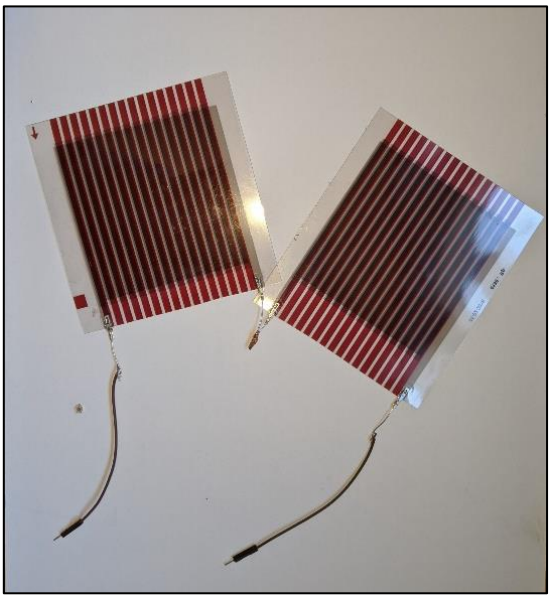

Figure 51. Printed Perovskite cells developed by Technical Research Centre of Finland (VTT).

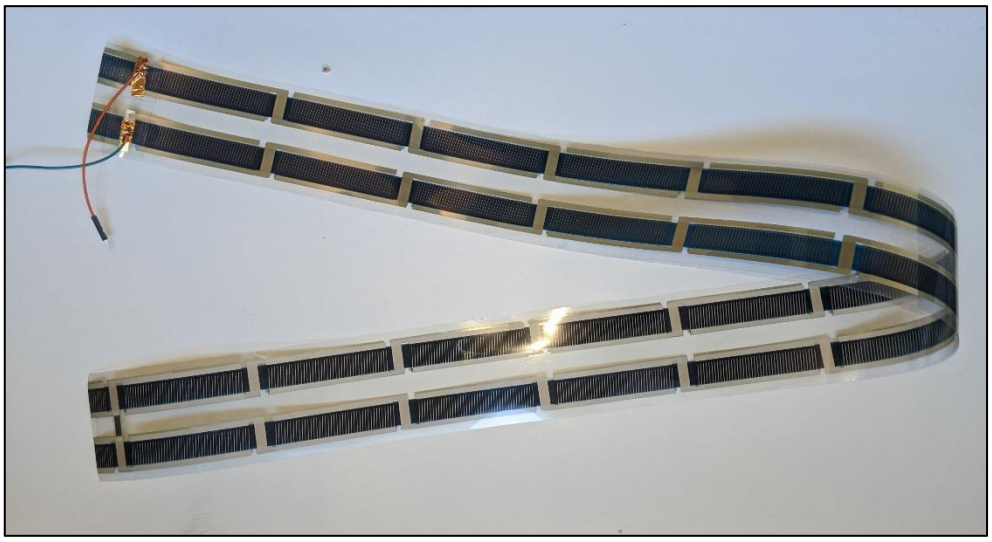

Figure 52. Printed organic PV cells developed by infinity PV.

6.3.1 Frequency response of designed system

The prototype's ability of responding to different frequencies were tested using square wave signals. To calculate signal to noise ratio (SNR) from received waveform, the following equation is used.

$$SNR = 20 * \log_{10}\left(\frac{Signal\ voltage}{Noise\ floor\ voltage}\right). \quad (30)$$

In the experiment, transmitter was placed 0.2m directly above the PV panels and performance both types of PV cells were tested. The results obtained are shown in Figure 53.

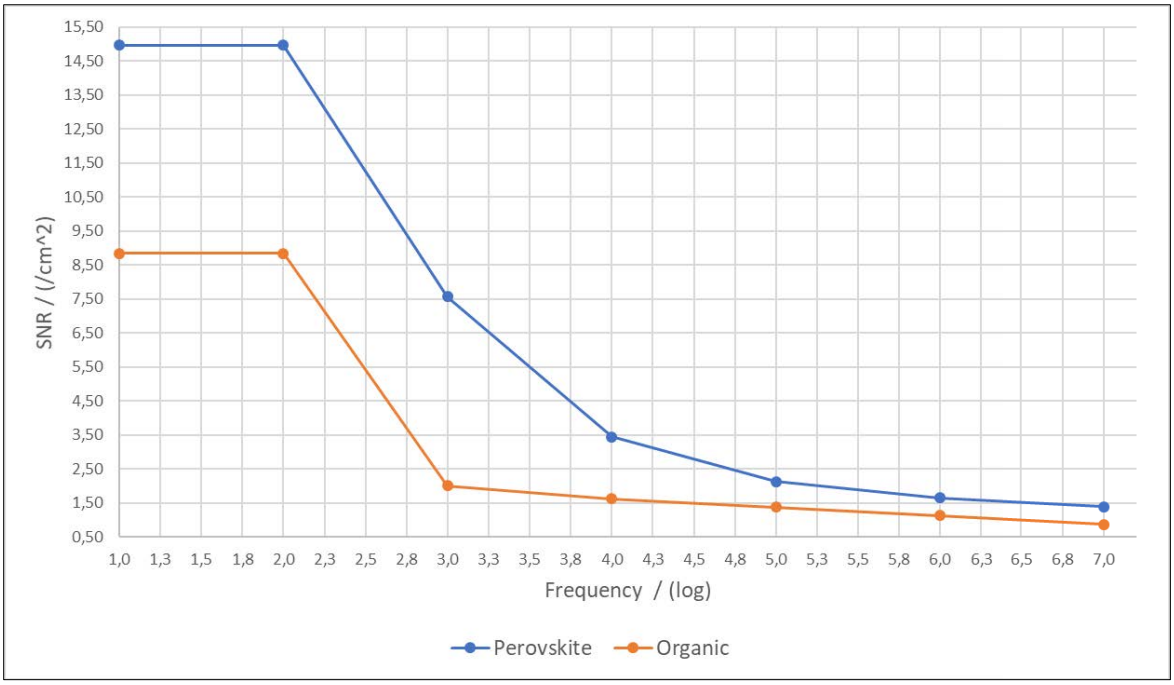

Figure 53. Frequency vs SNR variation of Perovskite and organic cells.

According to the graph, it can be clearly observed that the SNR decreases with the increasing frequency. As both PV cells respond in a similar way it can be concluded that this is due to the slow frequency response limitation in the printed PV cells. According to [60] this behaviour can be also occurred due to the ratio between rise-fall time to the period of the pulse. The period of pulse is varying subjected to the frequency while the rise-fall rate is constant for the used transmitter LEDs and driver. Due to lack of pulse period, fall time and next pulse's rise time will tend to overlap. This phenomenon limits the voltage of the received data pulse which results a low SNR value. Oscilloscope-captured received distorted wave forms corresponding to the frequencies in Hz and kHz region can be observed in Figure 54 and 55 respectively.

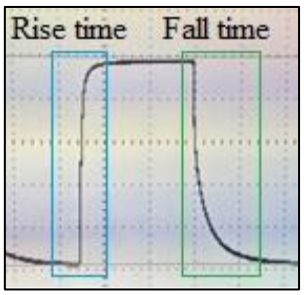

Figure 54. Pulse shape at Hz frequencies.

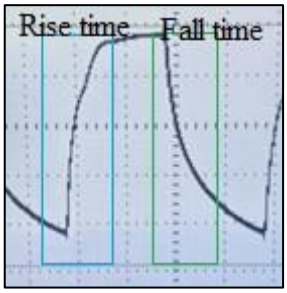

Figure 55. Pulse shape at kHz frequencies.

6.3.2 SNR variation with the distance.

For obtaining these results, the arrangement of measurement setup was as follows. At the initial experiment, setup was tested near a window where non direct sunlight interferes (300 lx). The transmitters were directly placed above the PV cells and then measurement was taken by changing the transmitting height in few steps.

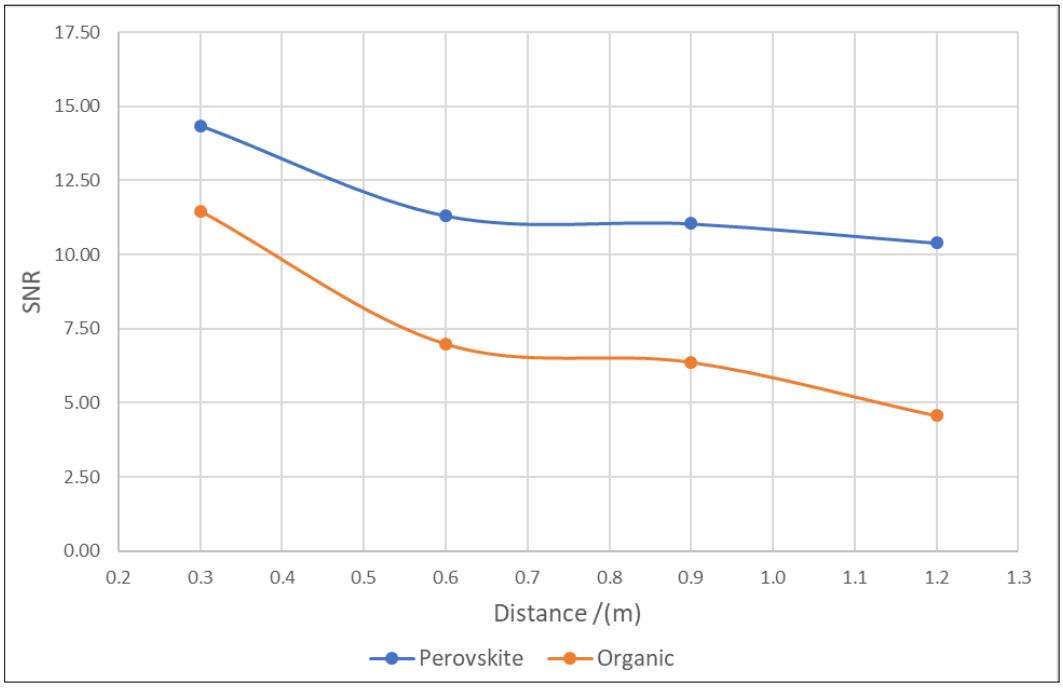

Figure 56. SNR variation with distance in an indoor sunlight environment.

The obtained results for experiment are plotted in Figure 56. According to the results the perovskite PV panel shows better performance compared to the OPV under indoor sunlight noisy scenario. The same experiment was repeated by only changing the noise environment. In this scenario, only the transmitters were used as the lighting sources resulting in a noise-free environment.

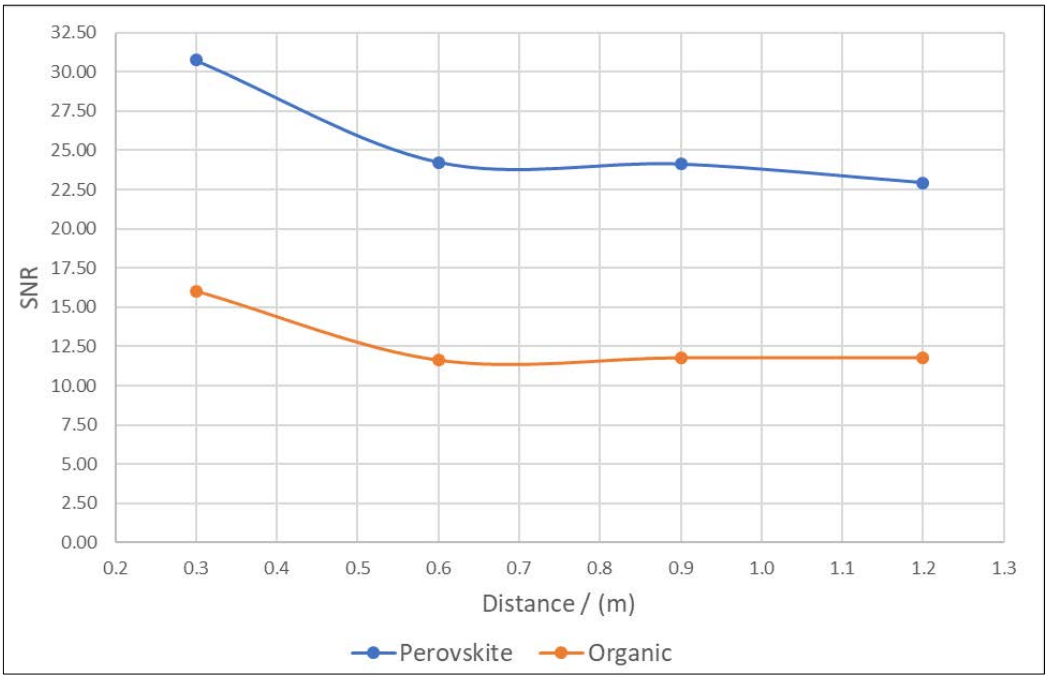

Figure 57. SNR variation with distance with only-transmitter illumination.

The results in Figure 57 suggests that this prototype will perform well under less noisy environment. Moreover, the results justified that the prototype can be used in noisy environments when the distance between transmitter and receiver is short.

6.4 Energy harvesting performance

In this prototype, the energy harvesting unit was directly powered by the PV cells. According to (20), the power conversion efficiency of a PV cell is directly proportional to the open circuit voltage when the terminal load is constant. Therefore, to measure the performance of the energy harvesting unit, open circuit voltage at the PV cell terminal were observed under different conditions. In this experiment, the prototype was placed under two transmitting schemes. Initially a set of readings were taken under the data transmitting scheme (flickering under PPM based REC80 protocol) conditions in the transmitter. Thereafter, the transmitter switched to idle transmitting scheme where no flicker occurs. The obtained results are depicted in Figure 58.

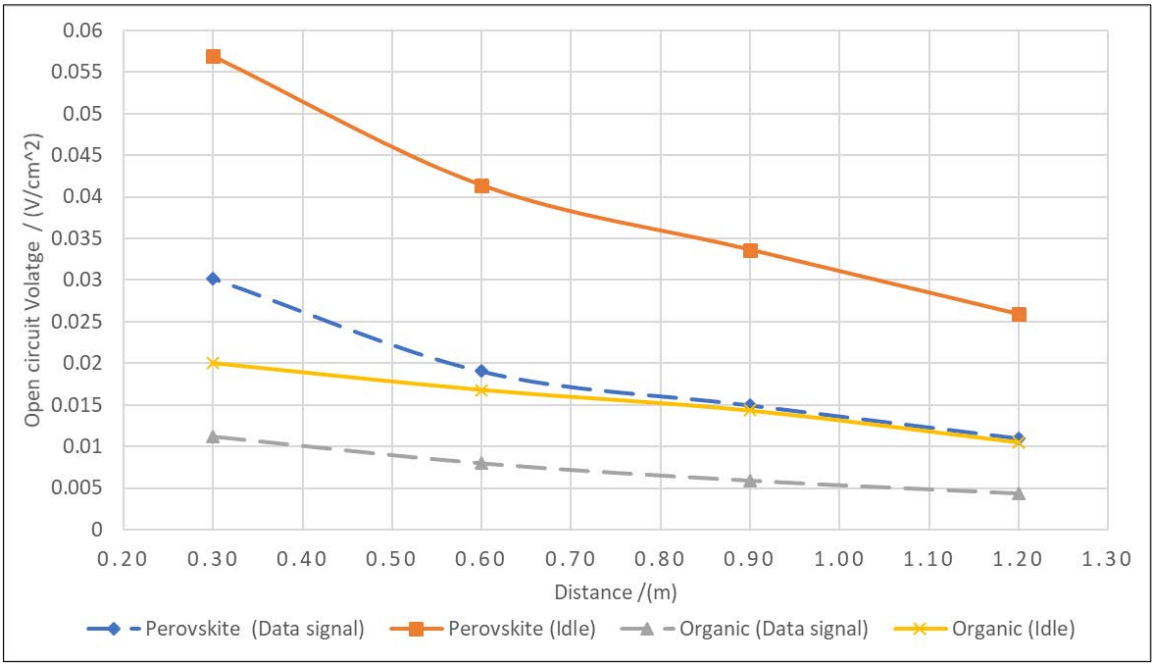

Figure 58. Energy harvesting scenario under two different transmitting schemes.

The results revealed that, the idle scheme generates significantly more voltage on the PV cells compared to the data transmitting mode. As the maximum power point of PV cell is based on the open circuit voltage in a given condition, it is important to use as large as possible open circuit voltage at the PV cells. This experiment proved the efficiency of transmitting algorithm implemented on transmitter hardware which was made to use both above discussed transmitting schemes.

6.4.1 Performance of energy harvesting unit

In this evaluation, performance between direct PV connection and through harvester IC connection were measured. The flowing current readings were obtained during transient booting phase of the microcontroller and steady operating conditions. The terminal voltage 6.5v was kept throughout the period. The results for the e-ink display based receiver are tabulated in Table 12.

Table 12: Maximum current readings for two different methods (e-ink based)

Phase	**Direct connection (max reading)**	**Energy harvesting IC based connection (max reading)**
Booting up phase	8 mA	4.20 mA
Steady operation phase	5.20 mA	3.80 mA

Based on the above results, it can observe that LTC 3588 harvesting IC drastically reduced by 47% the maximum drawing current during bootup phase while saving 27% of maximum drawing current during steady operating phase. The observed results for the electrochromic display-based receiver are tabulated in Table 13.

Table 13. Maximum current readings for two different methods (electrochromic based)

Phase	**Direct connection (max reading)**	**Energy harvesting IC based connection (max reading)**
Booting up phase	4.80 mA	3.10 mA
Steady operation phase	4.42 mA	3.00 mA

The results suggested that, the harvesting IC's algorithm managed to distribute the peak requirement of current along the time-axis with the help of the supercapacitor energy. This process effectively helped to reduce the PV voltage drop due to the series resistance in the PV cells by reducing the drawing current from the receiver circuit. In addition, results point out that, the printed flexible electrochromic displays have a better power efficiency when it compared to the other bi-stable display technologies.

7 DISCUSSION

The design, implementation and performance evaluation of a light-based IoT node was reported in this thesis. The hardware of transmitter unit was mainly selected and designed to facilitate the required data transmission rate for the chosen PPM based RECS 80 protocol. As suggested in Table 3 in literature review, that there are many VLC compatible modulation schemes which can be applied for this work. The ability of keeping constant signal waveform envelop in colour shift keying modulation, might be the best selection for both transmitting and energy generation application in this work. But from the power limited receiver design point of view, CSK's requirement of multiple signal detectors could have been difficult to achieve under the power constrains. Since the prototype is based on a novel concept, the prototype could have been made more effectively if it configured with innovative protocol specially designed for LIoT. As the RECS 80 protocol was originally designed for IR communication, in this case it only complied with the data transmission requirement of the prototype. In addition, the RECS 80 protocol is lacking an error detection mechanism compared to other IR technologies such as NEC protocol. The application used with the prototype, which sends text characters and graphics, is highly vulnerable to the erroneous transmission which, a fact that emphasise the requirement of error detecting mechanisms for detecting any possible transmission errors. However, to cater the all possible requirements for LIoT node, the protocol was retrofitted with addition of idle transmitting mode in order to give high intensity light for the energy harvesting. Figure 58 confirms the high energy generation in PV cells under the introduced idle transmitting scheme. In addition, the selection of COB as the light sources in the transmitter resulted in a new challenge. In transmitter's lighting source, the large number of compact LEDs in the COB create large heat dissipation which need to be separately addressed. This issue can be addressed by adding a heat sink with cooling fins on top of the transmitter, but it will make the design physically larger, questioning the selection criteria of COB for compact transmitter. However, by considering the factors such as well-directed light radiation pattern for the application, high light density and less complex connecting mechanism, the COB LEDs were selected for the design. The selection of cool white (5700K) as the transmitter's light colour was mainly based on the its positive effect on photovoltaic generation. However due to that, the applications of this prototype design will be limited to the selected light colour as other common indoor lighting colours such as warm white (< 4500K) are performing poorly on printed PV cells. The LED driver unit was properly biased to get better modulation bandwidth with better modulation index. As the result of that the transmitter was able to reach the required 38 kHz rate of LED transmission. A program script for the transmitter was written to cater the all the requirements of the prototype, such as input serial communication, ASCII to binary conversion, data transmitting and idle transmitting schemes.

The receiver was mainly prioritized for low energy consumption. To receive the VLC signal, photodiode-based receiver and PV cell-based receiver were tested. Since the surface area of the photodiode is small, the photodiode needed to be perfectly aligned to the lighting source in order to receive better SNR. This can be rectified to some extent by using special lenses arrangement in order to converge the lighting rays into the surface of photodiode area. In addition, fine-tuned AGC amplifier can be used to get constant signal power levels for the detecting purposes. On the other hand, since the PV cell units have large PV surface area, a cell has the ability to receive the incoming visible light without any special arrangement. In the PV cell-based design, the precision of received data signal extraction from the DC voltage can improved by adding higher order bandpass filtering. However, according to Figure 53, since the PE based PV cells are not capable of receiving 38 kHz frequency signals, the modulation

frequency of the design needs to be reduced. The e-ink display unit which was tested at the prototype design was not well complying with the low power design theme. The additional multipurpose display driver consumed more power than expected. As a solution for this, driverless display technologies like electrochromic display can be used. However, the ability of displaying multicharacter fonts and graphics in e-ink display was well ahead compared to the basic seven segment display which is electrochromic displays so far achieved. The ability of displaying multicharacter fonts and graphics were well matched with the purpose of the LIoT node.

In this thesis work, the energy harvesting design was tested by using two main approaches. In first approach the printed PV cells were directly connected to the circuit. As downside of this approach, the direct connection between PV cells and load caused the voltage to largely decrease due to the large current absorption from the load. To keep the required terminal voltage between the load, multiple PV cells were needed to use. This made the prototype much larger and practically not feasible due to the large surface area of the PV cells. Based on this method, it can be concluded that currently existing printed PV cells are not up to directly handling the current requirement. To mitigate this issue, in secondary approach, energy harvester purpose optimized IC based setup used. This harvesting circuit isolated the direct connection between the PV cells and load which resulted better terminal voltage using less PV cells. However, the power storage circuit components in the IC based harvesting circuit were directly challenged the design concept of "expose and connect" by keeping circuit alive even it is removed from the transmitter lights. In addition, due to the large charging time of super capacitors, the initial charging time was higher. It is necessary to point out that between this charging time the node will not be in operating mode. However, the results in Table 12 point out that the IC managed to reduce up to 25mW of the input power under 6.5v which was very effective on PV cells performance. Moreover, the harvesting IC made the protype more compact and more practical design due to low requirement of PV surface area for the energy generation. As a part of feasibility checking on PV cell's compatibility for signal detection, two printed PV technologies were tested. The results demonstrated that the gravure printed perovskite cells have more voltage sensitivity to the typical indoor light compared to the printed organic cells. Based on that it can be concluded that perovskite cells can be used to produce further compact flexible designs due to its higher voltage sensitivity on small surface area. Generally, the power optimization criteria of the receiver nodes were constrained with the use of multipurpose electronic hardware's such as general development boards, outdoor light tuned PV cells and supporting electronic drivers which were equipped with unnecessary power consuming features for this task.

8 CONCLUSION AND FUTURE WORK

Throughout the work of this thesis the feasibility study and implementation of energy autonomous LIoT node were considered. As a proof of concept and to support and evaluate the performance of the concept, a prototype system with transmitter and multiple receiver nodes were developed. As the outcome of the thesis work, results were positive and each sperate segment of the prototype met the desired expectations. The transmitters and receivers were designed to facilitate the broadcast network architecture while supporting the multiuser requirements. The VLC unit proved that it is feasible to provide faster communication for the IoT nodes while providing sufficient light intensity for the PV based energy harvesting. Furthermore, the study carried out proved that printed electronics technology can be effectively used for the applications and PE technology is developed enough for meet the expectation from their applications.

As a future extension of this work, there are several research lines to be explored. As current receiver units are limited to broadcast type communication, checking the feasibility of integrating uplink will be important for future applications. Technologies like low power consuming IR uplink or retro reflector-based uplink integration could be applied to the current developed nodes. With these uplinks, LIoT user will have the ability to get feedback from the deployed nodes and use it for various customized applications. The MCU's power consumption could have been further optimized by using techniques such as introducing sleep modes, use of power-reduction registers, and run low power internal oscillators which are already available with the MCU. The receiver can be woken up from the sleep mode by using novel VLC waking up signalling scheme, just before sending the data signal from the transmitter. A combination of high illumination output from idle transmitting scheme at transmitter and low power consumption sleeping mode at receiver will provide more faster power storage at the super capacitors. Hence, as a future work, introducing sleeping mode to the prototype will be promising modification for further improve the power consumption. This can be implemented by introducing novel data transmission protocol with wake-up signalling for the LIoT nodes. More additional features like error detecting mechanism and multiuser addressing schemes can be integrated for the novel protocol. Furthermore, the transmitter prototype can be further improved to increase the node to transmitter distance. To achieve that lens arrangement can be used to provide more focused light beam towards the nodes while giving sufficient illumination for the indoor. In this way, this technology will be practically implemented on already existing infrastructures such as supermarkets, shopping malls etc. In future, by further improving the discussed suggestions and developments, this novel concept can be considered as a promising candidate for 6G-enabled Internet of Things.

9 REFERENCES

[1] H. Haas, “LiFi is a paradigm-shifting 5G technology,” *Reviews in Physics,* vol. 3, pp. 26-31, 2018.

[2] CISCO, “CISCO Visual Networking Index: Global Mobile Data Traffic Forecast Update,” CISCO, 2016-2021.

[3] Carsten Bockelmann, Nuno Pratas, Hosein Nikopour, Kelvin Au, Tommy Svensson, Cedomir Stefanovic, Petar Popovski, Armin Dekorsy, “Massive Machine-Type Communications in 5G: Physical and MAC-Layer Solutions,” in IEEE communications magazine, September, 2017.

[4] H. Haas, “Introduction to indoor networking concepts and challenges in LiFi,” Journal of Optical Communications and Networking, vol. 12, no. 2, p. A190, 2019.

[5] Mohanad Obeed, Anas M Salhab, Mohamed-Slim Alouini, Salam A Zummo, “On Optimizing VLC Networks for Downlink Multi-User Transmission: A Survey,” IEEE Communications Surveys & Tutorials, vol. 21, no. 3, pp. 2947-2976, 2019.

[6] Bangjiang Lin ; Xuan Tang ; Zabih Ghassemlooy ; Chun Lin ; Min Zhang ; Zhenlei Zhou ; Yi Wu ; Hui Li, “A NOMA scheme for visible light communications using a single carrier transmission,,” in 2017 First South American Colloquium on Visible Light Communications (SACVLC), Santiago, 2017.

[7] L. Chettri, “A Comprehensive Survey on Internet of Things (IoT) Toward 5G Wireless Systems,” IEEE Internet of Things Journal, vol. 7, no. 1, pp. 16-32, 2020.

[8] Hrishikesh Jayakumar, Arnab Raha, Younghyun Kim, “Energy-Efficient System Design for IoT Devices,” 2020.

[9] R. Vullers, “Micropower energy harvesting,” Solid-State Electronics, vol. 53, no. 7, pp. 684-693, 2009.

[10] Joseph Chang , Tong Ge, Edgar Sanchez-Sinencio, “Challenges of printed electronics on flexible substrates,” 2012 IEEE 55th International Midwest Symposium on Circuits and Systems (MWSCAS), pp. 582-585, 2012.

[11] H. Chun, “A Wide-Area Coverage 35 Gb/s Visible Light Communications Link for Indoor Wireless Applications,” Scientific Reports, vol. 9, no. 1, 2019.

[12] T. Perković, “BlinkComm: Initialization of IoT Devices Using Visible Light Communication,” Wireless Communications and Mobile Computing, pp. 1-16, 2018.

[13] M. Rasheduzzaman, P. B. Pillai, A. N. C. Mendoza and M. M. De Souza,, “A study of the performance of solar cells for indoor autonomous wireless sensors,” in 016 10th International Symposium on Communication Systems, Networks and Digital Signal Processing (CSNDSP), Prague, 2016.

[14] S. Zhang, “Organic solar cells as high-speed data detectors for visible light communication,” Optica, vol. 2, no. 7, p. 607, 2015.

[15] T. Rakia, “Optimal Design of Dual-Hop VLC/RF Communication System With Energy Harvesting,” IEEE Communications Letters, vol. 20, no. 10, pp. 1979-1982, 2016.

[16] Marcos Katz, Dominic O’Brien, “Exploiting novel concepts for visible light communications: from light-based IoT to living surfaces,” Optik - International Journal for Light and Electron Optics, October 2019.

[17] H. Haas, “High-speed wireless networking using visible light,” SPIE Newsroom, 2013.

[18] IEEE, “IEEE Standard for Local and metropolitan area networks--Part 15.7: Short-Range Optical Wireless Communications - Redline,” IEEE Std 802.15.7-2018 (Revision of IEEE Std 802.15.7-2011) - Redline , pp. 1-670, 23 April 2019.

[19] C. N, “ Outline,” in LED-Based Visible Light Communications, Berlin, Heidelberg, Springer, 2018.

[20] J. Vucic, “White Light Wireless Transmission at 200+ Mb/s Net Data Rate by Use of Discrete-Multitone Modulation,” IEEE Photonics Technology Letters, vol. 21, no. 20, pp. 1511-1513, 2009.

[21] C. N., “The Transmitter of the Visible Light Communication System,” in LED-Based Visible Light Communications., Signals and Communication Technology. Springer, Berlin, Heidelberg, 2018.

[22] N. C. N. Chi, “Ultra-high-speed single red–green–blue light-emitting diode-based visible light communication system utilizing advanced modulation formats,” Chinese Optics Letters, vol. 12, no. 1, pp. 010605-10608, 2014.

[23] S. M. BERMAN, “Human Electroretinogram Responses to Video Displays, Fluorescent Lighting, and Other High Frequency Sources,” Optometry and Vision Science, vol. 68, no. 8, pp. 645-662, 1991.

[24] P. C. S. M. Amna Aljaberi, “Modulation Schemes for Visible Light,” in 2019 International Conference on Advanced Communication Technologies and Networking (CommNet), Rabat, Morocco, 2019.

[25] Trio Adiono, Syifaul Fuada, “Optical Interference Noise Filtering over Visible Light Communication System,” in 2017 International Symposium on Nonlinear Theory and Its Applications,, Cancun, Mexico, 2017.

[26] Y. Zhao, “Design of Visible Light Communication Receiver for On-Off Keying Modulation by Adaptive Minimum-Voltage Cancelation,” Engineering Journal, vol. 17, no. 4, pp. 125-130, 2013.

[27] Fu-Liang Chang, Wei-Wen Hu, Da-Huei Lee, Chao-Tang Yu, “Design and implementation of anti low-frequency noise in visible light communications,” in Proceedings of the 2017 IEEE International Conference on Applied System Innovation, 2017.

[28] C. N, “Visible Light Communication Post-equalization Technology,” in LED-Based Visible Light Communications, Springer, Berlin, Heidelberg, 02 September 201.

[29] Barry, J.R., Kahn, J.M., “Simulation of multipath impulse response for indoor wireless opticalchannels,” IEEE.

[30] C. N, “Models of the Visible Light Channel,” in LED-Based Visible Light Communications, Springer, Berlin, Heidelberg, 02 September 2018.

[31] I. B. Djordjevic, in Advanced Optical and Wireless Communications Systems, Springer International Publishing, 2018, pp. 180-195.

[32] S. &. H. &. M. M. &. M. &. S. R. Pervez, “LiFi: The Future for Indoor Wireless Data Communication,” International Journal of Scientific and Engineering Research, vol. 7, pp. 71-79, 2016.

[33] C.-C. Kao, “ A Comprehensive Study on the Internet of Underwater Things: Applications, Challenges, and Channel Models,” Sensors, vol. 17, no. 7, p. 1477, 2017.

[34] F. Wang, “High speed underwater visible light communication system based on LED employing maximum ratio combination with multi-PIN reception,” Optics Communications, vol. 425, pp. 106-112, 2018.

[35] N. C. N. Chi, “Advanced modulation formats for underwater visible light communications,” Chinese Optics Letters, vol. 16, no. 12, 2018.

[36] P. P. Jenkins, “High-Bandgap Solar Cells for Underwater Photovoltaic Applications,” IEEE Journal of Photovoltaics, vol. 4, no. 1, pp. 202-207, 2014.

[37] Y. Liu, “Lab-on-Skin: A Review of Flexible and Stretchable Electronics for Wearable Health Monitoring,” ACS Nano, vol. 11, no. 10, pp. 9614-9635, 2017.

[38] Z. Cui, “Printing practice for the fabrication of flexible and stretchable electronics,” Science China Technological Sciences, vol. 62, no. 2, pp. 224-232, 2019.

[39] Perelaer J, Schubert US, “Inkjet printing and alternative sintering of narrow conductive tracks on flexible substrates for plastic electronic applications,” in Flexible Electronics Handbook of Radio Frequency Identification Fundamentals and Applications Design Methods and Solutions. Croatia: InTech, 2010.

[40] F. C. J. Torrisi, “Electrifying inks with 2D materials,” Nature Nanotech , p. 738–739, 2014.

[41] Kelley T, Klauk H, “Materials, Manufacturing and Applications,” in Organic Electronics, Berlin:, Wiley,, 2006.

[42] [. D., “Nanomaterials are becoming synonymous with printed electronics.,” Printed Electronics Now, 2011.

[43] Sekitani T, Zschieschang U, Klauk H, “Flexible organic transistors and circuits with extreme bending stability,” p. 1015–1022, 2010.

[44] L. A. R. a. J. C. V. Sílvia Manuela Ferreira Cruz, “Printing Technologies on Flexible Substrates for Printed Electronics”.

[45] K. Suganuma, -Introduction to Printed Electronics page 30, Springer (2014) , 2014.

[46] Gans BJ, Duineveld PC, Schubert US, “State of the art and future developments,” Inkjet printing of polymers, pp. 203-213, 2004.

[47] “Printing processes and their potential for RFID printing,” Proceedings of the 2005 Joint Conference on Smart Objects and Ambient Intelligence:Innovative Context-Aware Services: Usages and Technologies. Grenoble, France: ACM;2005. pp. 27-30.

[48] Y. Chung, A. Li, J. Lee, H. Fang and C. Tsai, , “"Electrochromic device with full-color technology," 2010 23rd Annual Meeting of the IEEE Photonics Society, Denver,,” pp. 250-251, 2010.

[49] A. Abdelnour, A. Hallet, S. B. Dkhil, P. Pierron, D. Kaddour and S. Tedjini,, “Energy Harvesting Based On Printed Organic Photovoltaic Cells for RFID Applications,” in 2019 IEEE International Conference on RFID Technology and Applications (RFID-TA),, Pisa, Italy, 2019.

[50] K. Kalyanasundaram., Dye-sensitized solar cells, Switzerland: EPFL Press (CRC Press), 2010.

[51] Open circuit voltage of organic solar cells: an in-depth reviewreview, “Naveen Kumar Elumalai,” Energy & Environmental Science, vol. 9, no. 2, pp. 391-410.

[52] Martin A. Green Yoshihiro Hishikawa Ewan D. Dunlop Dean H. Levi Jochen Hohl-Ebinger Anita W.Y. Ho-Baillie, “Solar cell efficiency tables (version 52),” 19 June 2018.

[53] Young Yun Kim, Tae-Youl Yang, Riikka Suhonen, Marja Välimäki, Tiina Maaninen,, “Gravure-Printed Flexible Perovskite Solar Cells: Toward,” advancedscience, 2019.

[54] Teng-ChunWuYean-SanLongShu-TsungHsuEn-YunWang, “Efficiency Rating of Various PV Technologies under Different Indoor Lighting Conditions,” in Proceedings of the SNEC 11th International Photovoltaic Power Generation Conference & Exhibition, SNEC 2017 Scientific Conference, September 2017, Pages 66-71.

[55] Perm Soonsawad, Kang Eun Jeon, James She, Ching Hong Lam and Pai Chet Ng, “Maximizing Energy Harvesting with Adjustable Solar Panel for BLE Beacon”.

[56] Y. Li, N.J. Grabham, S.P. Beeby, M.J. Tudor, “The effect of the type of illumination on the energy harvesting performance of solar cells,” Elsevier, January 2015.

[57] L. A. Andrew Kring, “Spectroscopy”.university of Georgia, Athens, Georgia 30602.

[58] C. XLamp®, “ CXA2540 LED Datasheet”.

[59] “electronics-tutorials,” [Online]. Available: https://www.electronics-tutorials.ws/rc/rc_1.html.

[60] Angga Pradana, Nur Ahmadi, Trio Adiono, Willy Anugrah Cahyadi, Yeon-Ho Chung, "VLC Physical Layer Design based on Pulse Position," 2015 International Symposium on Intelligent Signal Processing and Communication Systems (ISPACS) , November 9-12, 2015.

10 APPENDICES

Appendix 1: BER checking algorithm

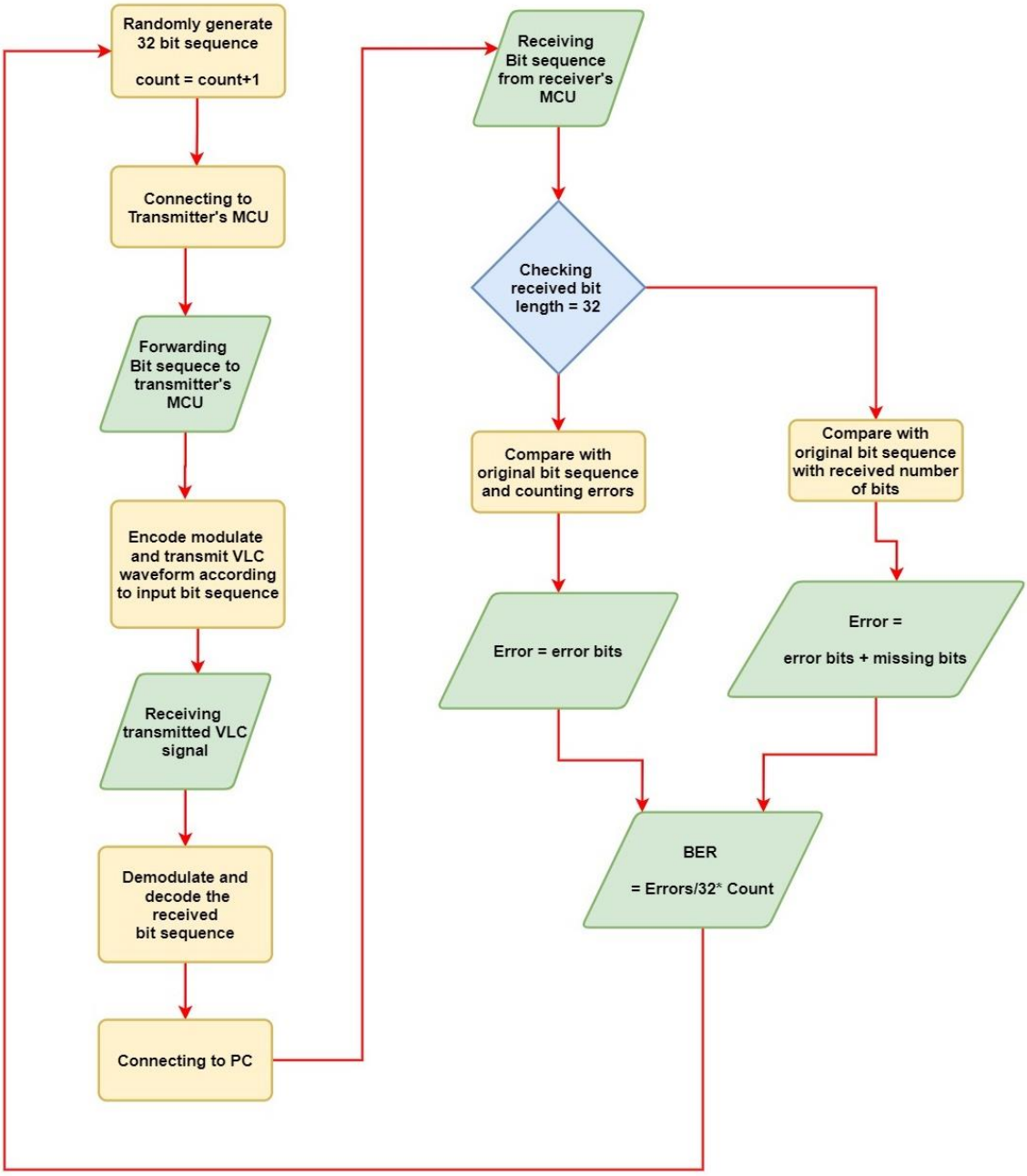

Figure 59. Algorithm used for BER calculation

Appendix 2: Transmitter schematics

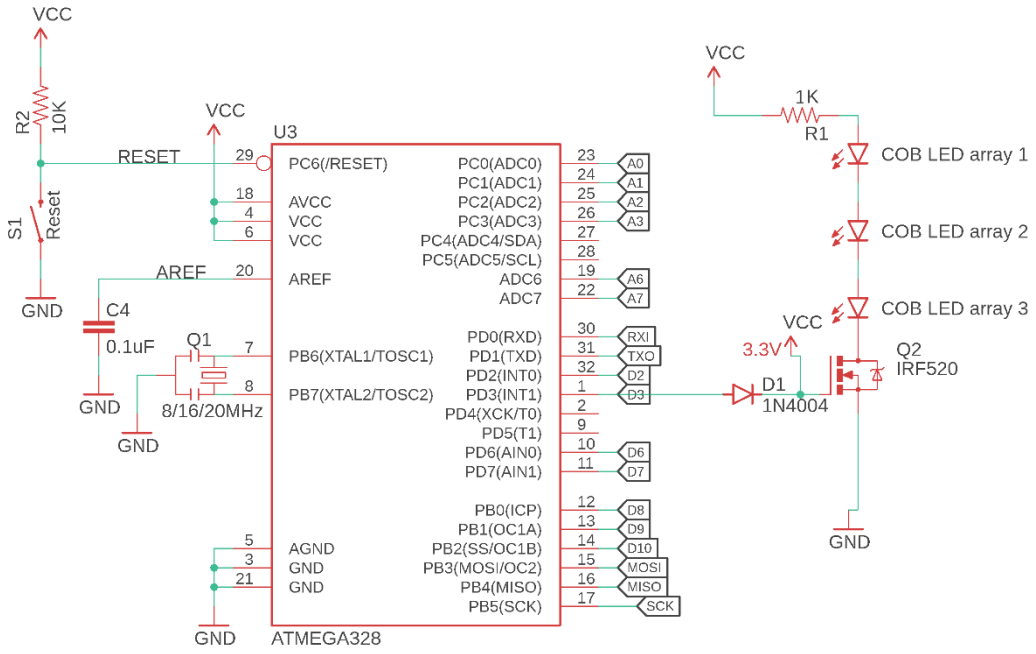

Figure 60. Transmitter unit design schematics

Appendix 3: Receiver design schematics

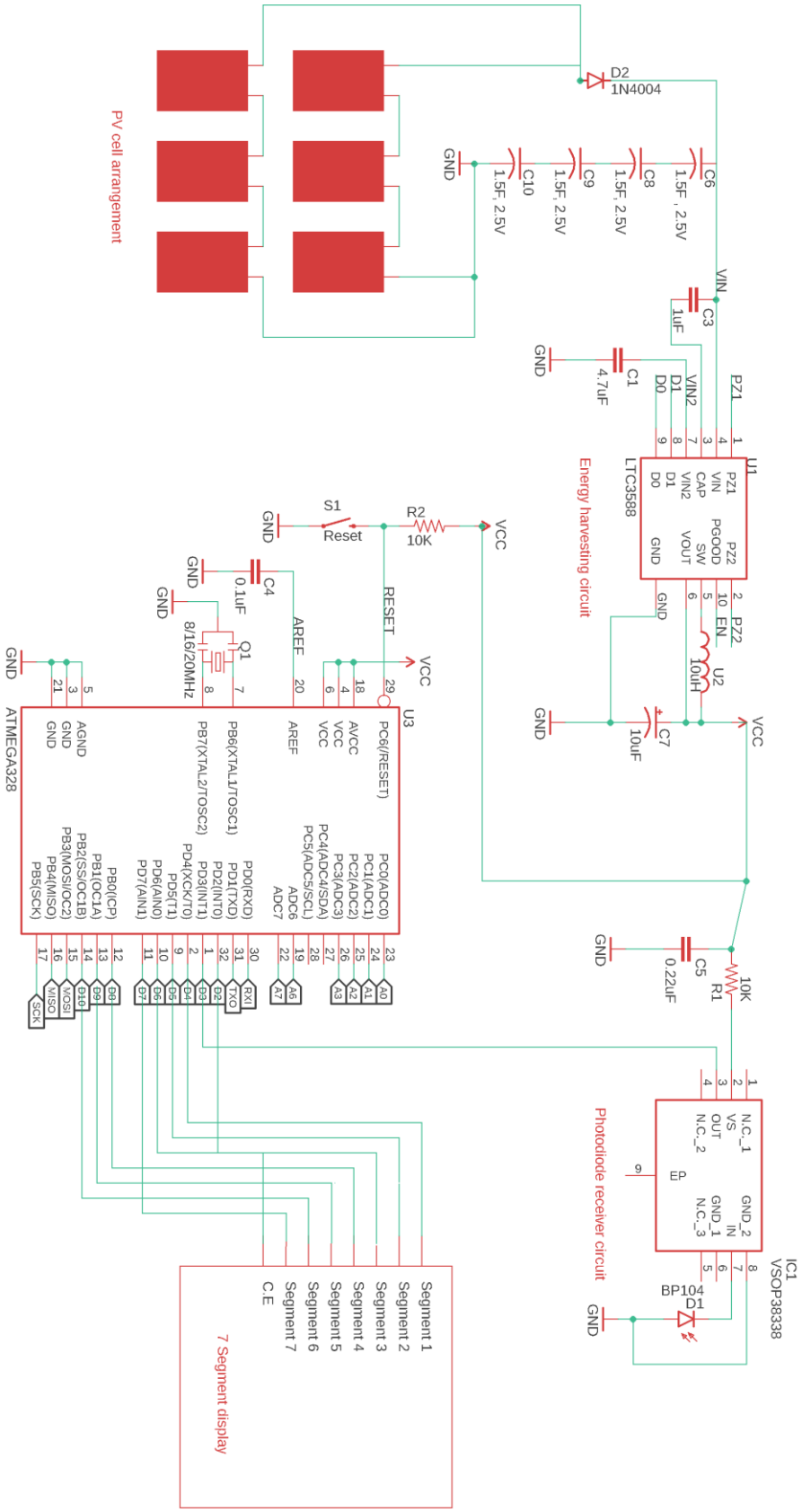

Figure 61. Receiver design schematics